

Color Superconductivity of QCD at High Baryon Density ^{*}

Hai-cang Ren [†]

Physics Department, The Rockefeller University 1230 York Avenue, New York, NY 10021-6399

Abstract

At sufficiently high baryon density, a quark matter is expected to become a color superconductor because of the pairing forces mediated by gluons. The theoretical aspect of this novel phase of the strong interaction is reviewed with the emphasis on the perturbation theory of QCD at high chemical potential and low temperature. The derivation of the scaling formula of the superconducting transition temperature at weak coupling is explained in detail. The Ginzburg-Landau theory of the color superconductivity is also discussed.

Typeset using REVTEX

^{*}Lecture notes at the domestic workshop "Progresses in Color Superconductivity" of China Center of Advanced Science and Technology (CCAST), Beijing, China, Dec 8-Dec 11, 2003.

[†]E-mail: ren@summit.rockefeller.edu

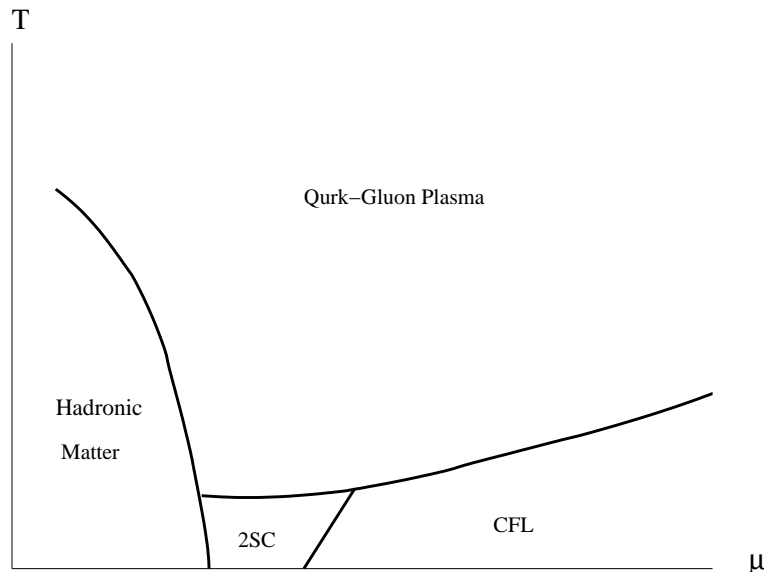


FIG. 1. The phase diagram of QCD.

I. INTRODUCTION

The properties of quantum chromodynamics, QCD, at nonzero temperature and nonzero baryon density have become a active area of research involving both high energy physicists and nuclear physicists. The asymptotic freedom of QCD is expected to release its fundamental degrees of freedom, quarks and gluons, from the color confinement under these extreme conditions. New new phases of the strong interaction, the quark-gluon plasma (QGP) at high temperature and the color superconductivity (CSC) at high baryon density [1] [2] [3] [4] [5] [6] will emerge. The speculated phase diagram of QCD is shown in Fig.1. There are two phases of the color superconductivity, 2SC and CFL. The former corresponds to Cooper pairing among the two flavors of quarks, u and d , while s quark is too massive to participate. The latter occurs at higher chemical potential and involves s in Cooper pairing with the ground state color-flavor locked [6].

Experimentally, the QGP phase may be reached by colliding two heavy nuclei at sufficiently high energy. The recent discovery of the jet quenching effect in gold-gold collisions versus deuteron-gold collisions at RHIC (Relativistic Heavy Ion Collider) suggests that such a novel phase might have been produced post gold-gold collisions [7]. The color superconductivity phase, though not likely to be created at RHIC, is speculated to exist inside a compact stellar object, say a neutron star. Its observational aspects, however, is still primitive at this time.

Considerable theoretical endeavors have been expended in past years to explore different regions of the QCD phase diagram. Along the temperature axis or slightly off it with a small chemical potential, accumulated results of lattice simulation of QCD have reached a consensus that a deconfinement phase transition, accompanied by the restoration of chiral symmetry, occurs at $T \simeq 150$ MeV. But present methodology of lattice simulation become inadequate when the chemical potential becomes large because of the fermion sign problem. On the other hand, the pairing instability that underlying the color superconducting phase

transition extends to an arbitrarily high chemical potential and perturbative techniques are available when the chemical potential becomes much higher than Λ_{QCD} . First principle calculations have been made along this line and the scaling formula relating the transition temperature or the energy gap to the chemical potential and the running coupling constant of QCD has been derived systematically [8] [9] [10] [11] [12] [13] [14] [15] [16] [17] [18] [19]. Even though the condition for the perturbative treatment may not be implemented in nature, these result serves a rigorous proof as to the existence of the color superconducting phase of QCD at sufficiently high baryon density. The region of moderate baryon density, which represents the most interesting case from the observational prospect, is unfortunately too difficult to warrant a first principle investigation with present analytical and numerical techniques. One is compelled to resort to various effective actions a la Nambu-Jona-Lasinio, regarding the parameters involved phenomenological.

In this lecture, I will focus on the color superconducting phase of QCD, especially its perturbative region. Several salient features of the color superconductivity will be summarized in the next section. A perturbation theory of CSC at ultra high chemical potential, along with the derivation of the scaling formula of the transition temperature, will be re-reviewed in sections III and IV. A nontrivial application of the perturbation theory to the crystalline color superconductivity will be presented in section V. Section VI is devoted to the Ginzburg-Landau theory of the color superconductivity, which is less correlated to other sections. Some outlooks of the field together with comments on higher order corrections and non-standard pairing possibilities are presented in the final section. As only selected topics are discussed in this lecture, the interested readers are recommended to consult more comprehensive review articles in the literature [20] for the materials not covered here.

II. THE COLOR SUPERCONDUCTIVITY OF QCD.

A. The pairing forces in QCD.

The thermodynamics of a quark matter at nonzero temperature T and nonzero baryon density is described by QCD Lagrangian with a Euclidean time $0 < \tau < \beta$, $\beta = (k_B T)^{-1}$ and a nonzero chemical potential μ

$$\mathcal{L} = -\frac{1}{2} \text{tr} F_{\mu\nu}^l F_{\mu\nu}^l - \bar{\psi} \left(\frac{\partial}{\partial x_\mu} - ig A_\mu \right) \psi + \mu \bar{\psi} \gamma_4 \psi - \bar{\psi} m \psi + \text{renormalization counter terms}, \quad (2.1)$$

where $A_\mu = A_\mu^l T^l$, $F_{\mu\nu} = \frac{\partial A_\nu}{\partial x_\mu} - \frac{\partial A_\mu}{\partial x_\nu} - ig [A_\mu, A_\nu]$ with T^l the $SU(N_c)$ generator in its fundamental representation, and ψ is a Dirac spinor with both color and flavor indices. The mass matrix m of quarks is diagonal with respect flavor indices. The chiral limit $m \rightarrow 0$ is assumed throughout the lecture except in the sections V and VII when exotic pairing states are considered. The renormalized coupling constant appropriate for low temperature and high density is given by the running coupling constant evaluated at the chemical potential, i.e.

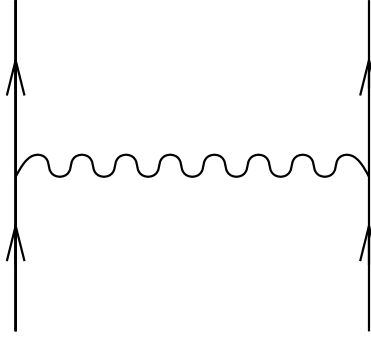


FIG. 2. The one-gluon exchange vertex.

$$g = \frac{24\pi^2}{(11N_c - 2N_f) \ln \frac{\mu}{\Lambda_{\text{QCD}}}}, \quad (2.2)$$

where $N_f < \frac{11}{2}N_c$ and $\mu \gg \Lambda_{\text{QCD}}$. Although $N_c = 3$ for QCD, most of the formulations developed are valid for arbitrary N_c . We shall not fix the value of N_c unless it is necessary, say in the context of the pairing symmetry in the superconducting phase.

Perturbatively, the diquark interaction is dominated by the process of one-gluon exchange, as is shown in Fig. 2. The amplitude is simply that of the one-photon exchange in QED multiplying the group theoretic factor $T_l^{c'_1 c_1} T_l^{c'_2 c_2}$, which can be decomposed into a color anti-symmetric channel (anti-triplet for $SU(3)$) and a color symmetric one (sextet for $SU(3)$) [3], i.e.

$$T_l^{c'_1 c_1} T_l^{c'_2 c_2} = -\frac{N_c + 1}{4N_c} (\delta^{c'_1 c_1} \delta^{c'_2 c_2} - \delta^{c'_1 c_2} \delta^{c'_2 c_1}) + \frac{N_c - 1}{4N_c} (\delta^{c'_1 c_1} \delta^{c'_2 c_2} + \delta^{c'_1 c_2} \delta^{c'_2 c_1}) \quad (2.3)$$

As both the electric and magnetic parts of the one-photon exchange are repulsive between two electrons flying in opposite directions, the one-gluon exchange interaction between two quarks flying in opposite directions is attractive in the color anti-symmetric channel because of the negative sign of the group theoretic factor (first term on r. h. s. of (2.3)).

The formula (2.3) can be generalized to the two quarks in arbitrary irreducible representations R_1 and R_2 of the gauge group and we have

$$(T_{R_1}^l)^{c'_2 c_2} (T_{R_2}^l)^{c'_1 c_1} = \sum_{R \subset R_1 \otimes R_2} G(R|R_1, R_2) \mathcal{P}^{c'_1, c'_2; c_1, c_2}(R|R_1, R_2) \quad (2.4)$$

with the group theoretic factor

$$G(R|R_1, R_2) = \frac{1}{2}(C_R - C_{R_1} - C_{R_2}), \quad (2.5)$$

where C_R is the second Casimir of the representation R and $\mathcal{P}(R|R_1 \otimes R_2)$ projects out the irreducible representation R out of $R_1 \otimes R_2$ and satisfies

$$\mathcal{P}^{c'_1, c'_2; c''_1, c''_2}(R'|R_1, R_2) \mathcal{P}^{c''_1, c''_2; c_1, c_2}(R|R_1, R_2) = \begin{cases} \mathcal{P}^{c'_1, c'_2; c_1, c_2}(R|R_1, R_2) & \text{for } R' = R \\ 0 & \text{for } R' \neq R \end{cases}. \quad (2.6)$$

The channel with negative $G(R|R_1, R_2)$ is attractive. The derivation of (2.4) is shown in Appendix A.

Another pairing force, which is expected to dominate at moderate baryon density, stems from the instanton-induced interaction among light quarks discovered by 't Hooft [21]. For two quark flavors, it is of NJL type and reads [5]

$$\begin{aligned} \mathcal{L}_{\text{eff.}} = G \Big\{ & -\frac{1}{8N_c^2(N_c-1)} [(\tilde{\psi}C\tau_2T_A^l\psi)(\bar{\psi}\tau_2T_A^lC\tilde{\psi}) + (\tilde{\psi}C\tau_2T_A^l\gamma_5\psi)(\bar{\psi}\tau_2T_A^l\gamma_5C\tilde{\psi})] \\ & + \frac{1}{16N_c^2(N_c+1)} (\tilde{\psi}C\tau_2T_S^l\sigma_{\mu\nu}\psi)(\bar{\psi}\tau_2T_S^l\sigma_{\mu\nu}C\tilde{\psi}) \Big\}, \end{aligned} \quad (2.7)$$

where C is the charge conjugation matrix, $T_{A(S)}^l$ is proportional to $SU(N_c)$ generator in color antisymmetric (symmetric) channel and the second Pauli matrix τ_2 acts on isospin indices of ψ . The coupling strength $G > 0$ can be expressed explicitly in terms of the running coupling constant, the chemical potential and the critical chemical potential for chiral symmetry restoration [22]. Like one-gluon exchange, the pairing channel is also color antisymmetric.

B. The transition temperature and the energy gap at weak coupling.

Although the running coupling constant becomes weak for $\mu \gg \Lambda_{\text{QCD}}$, the infrared divergence, because of the long range propagation of magnetic gluons introduces complications to the perturbative expansion. Consequently, the scaling formula for the energy gap and the critical temperature differs remarkably from that of a BCS superconductor, which is driven by a short range pairing force via one-phonon-exchange. Through the efforts of several groups, the first-principle formula for the pairing temperature has been derived. It reads

$$k_B T_{\text{pair}}^{(J)} = cc'c''c_J \frac{\mu}{g^5} e^{-\frac{\kappa}{g}} [1 + O(g \ln g)], \quad (2.8)$$

where the coefficient of the non-BCS exponent

$$\kappa = \sqrt{\frac{6N_c}{N_c+1}} \pi^2 \quad (2.9)$$

was first obtained in [8], the pre-exponential factor

$$c = 1024\sqrt{2}\pi^3 N_f^{-\frac{5}{2}} \quad (2.10)$$

was found in [9] and [11], and the factor

$$c' = 2e^\gamma \quad (2.11)$$

with γ the Euler constant was found in [11] and [15]. The factor

$$c'' = \exp \left[-\frac{1}{16}(\pi^2 + 4)(N_c - 1) \right] \quad (2.12)$$

comes from the non Fermi liquid behavior of the quark self energy and was determined in [14] [18] (The existence of this correction was suggested in [8]). The angular momentum dependent factor c_J was derived in [15] and is given by

$$c_J = e^{-6s_J} \quad (2.13)$$

for equal helicity pairing with $J \geq 0$ and

$$c_J = e^{-6s'_J} \quad (2.14)$$

for cross helicity pairing with $J \geq 1$ where

$$s_J = \begin{cases} 0 & \text{for } J = 0 \\ \sum_{n=1}^J \frac{1}{n} & \text{for } J > 0 \end{cases} \quad (2.15)$$

and

$$s'_J = \frac{1}{2} \left(s_J + \frac{J}{2J+1} s_{J+1} + \frac{J+1}{2J+1} s_{J-1} \right). \quad (2.16)$$

The superconducting transition temperature T_c is the highest pairing temperature that is consistent with the pairing symmetry. We have $T_c = T_{\text{pair}}^{(J=0)}$ for pairing among different flavors and $T_c = T_{\text{pair}}^{(J=1)}$ for pairing within the same flavor [23].

The gap energy below T_c depends on the Matsubara frequency and reads

$$\Delta(\nu) \simeq \Delta_0 \sin \left(\frac{g}{2\pi} \sqrt{\frac{N_c+1}{6N_c}} \ln \frac{\mu}{|\nu|} \right) \quad (2.17)$$

at $T = 0$ and $|\nu| > \Delta_0$. Its maximum magnitude Δ_0 for $J = 0$ is related to T_c via

$$\frac{\Delta_0}{k_B T_c} = \begin{cases} \pi e^{-\gamma} & \text{for two flavor pairing} \\ 2^{-\frac{1}{3}} \pi e^{-\gamma} & \text{for color-flavor locking, } N_c = N_f = 3. \end{cases} \quad (2.18)$$

C. The pairing symmetry.

The gap parameter in the super phase, depending on the relative momentum, helicity, and color-flavor indices of pairing quarks, possesses rich structures under a spatial rotation or a transformation of the internal symmetry group

$$SU(3)_c \times SU(3)_R \times SU(3)_L \times U(1)_B \quad (2.19)$$

for three colors and three flavors in the chiral limit. To determine the energetically most favored pairing symmetry, we consider first the representation contents of color $SU(3)$ and flavor $SU(3)$, consistent with the signature under a simultaneous interchange of the color-flavor indices of the pairing quarks.

According to the angular momentum dependence of the pairing instability shown in the previous subsection, the most favorite diquark condensate should carry zero angular momentum and pair quarks of equal helicity and acquires a negative sign upon interchanging the

momenta and spins of the two quarks. Since the condensate should be antisymmetric with respect to interchanging all quantum numbers, the sign under a simultaneous interchange of their color-flavor indices ought to be positive, i.e.

$$\langle \psi_{f_2}^{c_2} \psi_{f_2}^{c_1} \rangle = \langle \psi_{f_1}^{c_1} \psi_{f_2}^{c_2} \rangle \quad (2.20)$$

If we define a $SU(3)$ rotation among flavor indices to be the conjugate of that among color indices, the representation contents of the diquark condensate are

$$(\bar{\mathbf{3}}_c, \mathbf{3}_f) \oplus (\mathbf{6}_c, \bar{\mathbf{6}}_f), \quad (2.21)$$

which can be decomposed further into a set of irreducible representations under a simultaneous $SU(3)$ rotation of both color and flavor indices. It was found in Ref. [6] that the condensate which minimize the free energy implements the unit representations of this diagonal $SU(3)$ rotation. This pairing symmetry is referred to as the color-flavor locking (CFL). The diquark condensate of CFL pairing takes the form

$$\langle \psi_{f_1}^{c_1} \psi_{f_2}^{c_2} \rangle = \phi_A (\delta_{f_1}^{c_1} \delta_{f_2}^{c_2} - \delta_{f_1}^{c_2} \delta_{f_2}^{c_1}) + \phi_S (\delta_{f_1}^{c_1} \delta_{f_2}^{c_2} + \delta_{f_1}^{c_2} \delta_{f_2}^{c_1}). \quad (2.22)$$

The two invariants $\phi_{A(S)}$ correspond to the two unit representation, one from each term of (2.21). The nonlinear coupling between these two unit representations makes $\phi_S \neq 0$ even though the pairing force is within the color antisymmetric channel. Both the gap equation [6] [24] and the Ginzburg-Landau theory [25] show that the magnitude of ϕ_S is suppressed relative to that of ϕ_A by one order of the expansion parameter involved and we shall come back to this point in section VI.

The CFL condensate breaks the symmetry (2.19) of QCD to

$$SU(3)_{c+R+L}(3) \times Z_2 \quad (2.23)$$

with $SU(3)_{c+R+L}$ standing for a simultaneous $SU(3)$ rotation of color indices, right hand flavor indices and left hand flavor indices. Like the standard model of electroweak interaction, it is possible to factor out a unbroken $U(1)$ group out of the electromagnetic $U(1)$, which is a subgroup of the flavor $SU(3)$, and one of $U(1)$ subgroup of the color $SU(3)$ [6] [26]. The gauge potential corresponding to this unbroken $U(1)$ plays to role of the electromagnetic field in the super phase. This, together with the energy gap, makes the physics of CFL condensate similar to that of an insulator regarding the new electromagnetism [27].

Since both right hand flavor indices and left hand ones are locked to the color indices. A spontaneous chiral symmetry breaking is thereby induced in the CFL condensate with the Goldstone bosons represented by the meson octet. The mass spectrum of the mesons in the presence of bare quark masses was computed in [28] [29] and they found that the order of the meson mass hierarchy are reversed from that in vacuum with η' the lightest member of the family.

III. THE PERTURBATION THEORY OF ONE GLUON EXCHANGE.

A. The perturbation theory of the transition temperature

The perturbative expansion of the pairing temperature refers to the expansion of $\ln \frac{\mu}{k_B T_{\text{pair}}}$ according to ascending powers of the running coupling constant g , i.e.

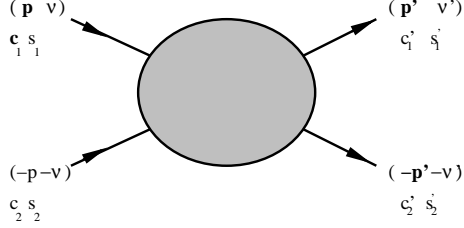


FIG. 3. Proper vertex function, $\Gamma_{s'_1, s'_2; s_1, s_2}^{c'_1, c'_2; c_1, c_2}(\nu', \vec{p}' | \nu, \vec{p})$.

$$\ln \frac{\mu}{k_B T_{\text{pair}}} = \frac{\kappa}{g} + \lambda + \lambda' g + O(g^2) \quad (3.1)$$

where the coefficients λ, λ', \dots may carry powers of $\ln g$. The $O(\frac{1}{g})$ term represents the leading order, the $O(1)$ term represents the sub-leading order and the $O(g)$ term represents the sub-sub-leading order and so on. It follows from (2.9) that $\kappa = \sqrt{\frac{6N_c}{N_c+1}} \frac{\pi^2}{g}$ and

$$\lambda = 5 \ln g - \ln(2048\sqrt{2}N_f^{-\frac{5}{2}}) - \gamma + \frac{(\pi^2 + 4)(N_c - 1)}{16} - \ln c_J \quad (3.2)$$

The derivation of (2.9) and (3.2) will be the main subject of the rest of this section and that of the coming section.

To generate the perturbation series (3.1) systematically, we start with the proper vertex function, Γ , corresponding to the scattering of two quarks with zero total energy and momentum. The Matsubara energies of incoming and outgoing quarks are denoted by $\pm\nu$ and $\pm\nu'$, respectively. Similarly, $\pm\vec{p}$ and $\pm\vec{p}'$ label the incoming and outgoing momenta. Each of the superscripts $c_i, i = 1, 2$, denote the color associated with each leg and the subscripts s , which label the states above or below the Dirac sea, are either $+$ or $-$. Primed variables are outgoing and unprimed incoming. This labeling scheme is illustrated in Fig. 10. Without special declaration, we shall reserve the Greek letters $\nu = 2\pi k_B T(n + 1/2)$ for the discrete Matsubara energy of a fermion and $\omega = 2\pi k_B Tn$ for that of a boson. The proper four-fermion vertex function satisfies a Schwinger-Dyson equation which, with all indices suppressed, may be written as,

$$\Gamma(\nu', \vec{p}' | \nu, \vec{p}) = \tilde{\Gamma}(\nu', \vec{p}' | \nu, \vec{p}) + \frac{1}{\beta} \sum_{\nu''} \int \frac{d^3 \vec{q}}{(2\pi)^3} K(\nu', \vec{p}' | \nu'', \vec{q}) \Gamma(\nu'', \vec{q} | \nu, \vec{p}), \quad (3.3)$$

where $\tilde{\Gamma}$ represents the two particle irreducible part (2PI) of a vertex diagram. The kernel has the explicit form,

$$K_{s'_1, s'_2; s_1, s_2}^{c'_1, c'_2; c_1, c_2}(\nu', \vec{p}' | \nu, \vec{p}) = \tilde{\Gamma}_{s'_1, s'_2; s_1', s_2'}^{c'_1, c'_2; c_1, c_2}(\nu', \vec{p}' | \nu, \vec{p}) \mathcal{S}_{s_1' s_1}(\vec{p} \nu) \mathcal{S}_{s_2' s_2}(-\vec{p} - \nu), \quad (3.4)$$

where $\mathcal{S}_{s' s}(\vec{p}, \nu)$ denotes the full quark propagator with momentum \vec{p} and Matsubara energy ν . In order to facilitate the partial wave analysis we found it convenient to associate the Dirac spinors $u(\vec{p})$ and $v(\vec{p})$, which satisfy the Dirac equations $(\gamma_4 p - i\vec{\gamma} \cdot \vec{p})u(\vec{p}) = 0$ and $(\gamma_4 p - i\vec{\gamma} \cdot \vec{p})v(\vec{p}) = 0$, to the quark-gluon vertex instead of to the quark propagator. Thus the vertices written in (3.3) are of the form,

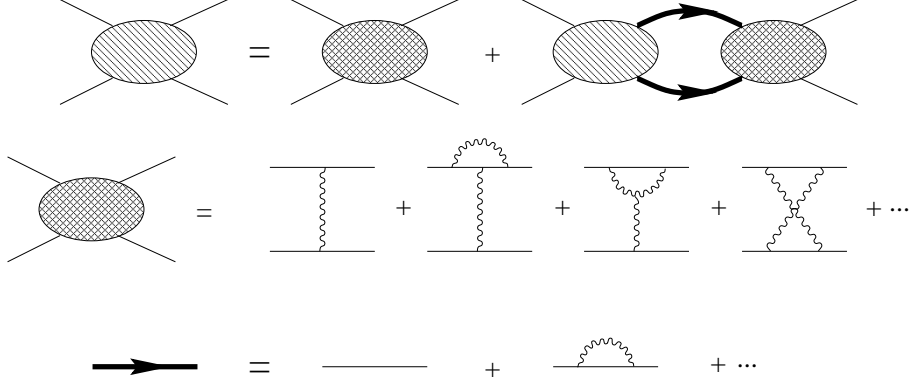


FIG. 4. The Schwinger-Dyson equation. Γ is represented by single hashed vertices and $\tilde{\Gamma}$ is represented by double hashed vertices. The full quark propagator is represented by a solid line and the bare quark propagator by a thin line. Gluon propagators, including hard thermal loops, are represented by curly lines. The first two orders in the expansion of $\tilde{\Gamma}$ and the full quark propagator are given.

$$\Gamma_{s'_1, s'_2, s_1, s_2} = \overline{U}_\gamma(s'_1, \vec{p}') \overline{U}_\delta(s'_2, -\vec{p}') \Gamma_{\gamma\delta, \alpha\beta} U_\alpha(s_1, \vec{p}) U_\beta(s_2, -\vec{p}), \quad (3.5)$$

with the vertex function $\Gamma_{\gamma\delta, \alpha\beta}$ given by conventional Feynman rules and $U(+, \vec{p}) = u(\vec{p})$ or $U(-, \vec{p}) = v(-\vec{p})$, respectively. However, since the quarks are massless, $\gamma_5 u = -u$ and $\gamma_5 v = -v$, to simplify notation we may identify $U(s, \vec{p}) = u(s\vec{p})$. The diagram of the Dyson-Schwinger equation, the first few diagrams of the $\tilde{\Gamma}_{\gamma\delta, \alpha\beta}$ and $\mathcal{S}_{s', s}(\nu, p)$ are displayed in Fig. 4

The next step is to decompose Γ into irreducible representations of $SU(N_c)$ by either symmetrization or antisymmetrization among the initial and final color indices. We have,

$$\begin{aligned} \Gamma_{s'_1, s'_2, s_1, s_2}^{c'_1, c'_2; c_1, c_2}(\nu', \vec{p}' | \nu, \vec{p}) &= \frac{1}{2} (\delta^{c'_1 c_1} \delta^{c'_2 c_2} + \delta^{c'_2 c_1} \delta^{c'_1 c_2}) \Gamma_{s'_1, s'_2, s_1, s_2}^S(\nu', \vec{p}', |\nu, \vec{p}) \\ &+ \frac{1}{2} (\delta^{c'_1 c_1} \delta^{c'_2 c_2} - \delta^{c'_2 c_1} \delta^{c'_1 c_2}) \Gamma_{s'_1, s'_2, s_1, s_2}^A(\nu', \vec{p}', |\nu, \vec{p}), \end{aligned} \quad (3.6)$$

For the pairing instability, we need only to focus on the attractive antisymmetric channel. Proceeding with the partial wave analysis, we expand $\Gamma_{s'_1, s'_2, s_1, s_2}^A(\nu', \vec{p}' | \nu, \vec{p})$ in terms of Legendre polynomials (for equal helicity pairing),

$$\Gamma_{s'_1, s'_2, s_1, s_2}^A(\nu', \vec{p}' | \nu, \vec{p}) = \sum_J (2J+1) \gamma_{s'_1, s'_2, s_1, s_2}^J(\nu', \vec{p}' | \nu, \vec{p}) P_J(\cos \theta). \quad (3.7)$$

with θ the angle between \vec{p} and \vec{p}' . Using a similar expression for $\tilde{\Gamma}_{s', s}^A(\nu', \vec{p}' | \nu, \vec{p})$, we derive from (3.3) the Dyson-Schwinger equation satisfied by $\gamma_{s'_1, s'_2, s_1, s_2}^J(\nu', \vec{p}' | \nu, \vec{p})$:

$$\begin{aligned} \gamma_{s'_1, s'_2, s_1, s_2}^J(\nu', \vec{p}' | \nu, \vec{p}) &= \tilde{\gamma}_{s'_1, s'_2, s_1, s_2}^J(\nu', \vec{p}' | \nu, \vec{p}) \\ &+ \frac{1}{\beta} \sum_{\nu'', s''_1, s''_2} \int_0^\infty dq K_{s'_1, s'_2, s''_1, s''_2}^J(\nu', \vec{p}' | \nu'', \vec{p}'', q) \gamma_{s''_1, s''_2, s_1, s_2}^J(\nu'', \vec{p}'' | \nu, \vec{p}), \end{aligned} \quad (3.8)$$

where the kernel $K_{s'_1, s'_2; s_1, s_2}^J$ has the form,

$$K_{s'_1, s'_2; s_1, s_2}^J(\nu', p' | \nu, p) = \frac{p^2 \tilde{\gamma}_{s'_1, s'_2; s''_1, s''_2}^J(\nu', p' | \nu, p)}{2\pi^2} \mathcal{S}_{s''_1 s_1}(p, \nu) \mathcal{S}_{s''_2 s_2}(p, -\nu). \quad (3.9)$$

The Dyson-Schwinger equation (3.8) is of the Fredholm type, the stability of whose solution is governed by the Fredholm determinant [31]

$$\begin{aligned} \mathcal{D} = \det(1 - K) &= 1 - \frac{1}{\beta} \sum_{\nu', s_1, s_2} \int_0^\infty dp K_{s_1 s_2, s_1 s_2}(\nu, p | \nu, p) \\ &+ \frac{1}{2\beta^2} \sum_{\nu, \nu'; s_1, s_2; s'_1, s'_2} \int_0^\infty dp \int_0^\infty dp' \begin{vmatrix} K_{s_1, s_2; s_1, s_2}(\nu, p | \nu, p) & K_{s_1, s_2; s'_1, s'_2}(\nu, p | \nu', p') \\ K_{s'_1, s'_2; s_1, s_2}(\nu', p' | \nu, p) & K_{s'_1, s'_2; s'_1, s'_2}(\nu', p' | \nu', p') \end{vmatrix} + \dots \end{aligned} \quad (3.10)$$

In terms of the eigenvalues, E_n , of the kernel, defined by the solutions of,

$$Ef_{s_1, s_2}(\nu, p) = k_B T \sum_{\nu', s_1, s'_2} \int_0^\infty dp' K_{s_1, s_2; s'_1, s'_2}^J(\nu, p | \nu', p') f_{s'_1, s'_2}(\nu', p'), \quad (3.11)$$

we have

$$\mathcal{D} = \prod_n (1 - E_n). \quad (3.12)$$

Since \mathcal{D} appears in the denominator of the solution to the Fredholm equation, its roots represent the formation of a Cooper pair of quarks at the transition point to the super phase. At weak coupling and sufficiently high temperature, all eigenvalues are small ($\sim g^2$). As the temperature is lowered some of the eigenvalues may cross one because of the Fermi sea and the attractive interaction. The pairing temperature at an angular momentum J , $T_{\text{pair}}^{(J)}$, is the highest temperature when the corresponding highest eigenvalue crosses one, i.e.

$$E_{\text{max.}}^{(J)} \Big|_{T=T_{\text{pair}}^{(J)}} = 1. \quad (3.13)$$

The superconducting transition temperature is the highest one among the pairing temperatures of different angular momentum, i.e.

$$T_c = \max(T_{\text{pair}}^{(J)}, \forall J) \quad (3.14)$$

For equal helicity pairing, we have $T_c = T_{\text{pair}}^{(J=0)}$.

The Fredholm determinant corresponds to the sum of closed diagrams and is formally gauge invariant. The scale parameter Λ_{QCD} of (2.2), however is gauge dependent. Such a dependence should be eliminated order by order upon matching the infrared region and the ultraviolet region of the diagrams. Since the uncertainty of Λ represents an order $O(g^2)$ correction to the running coupling constant (2.2), it contributes to the sub-sub-leading term of (3.1) and is beyond the scope of the present lecture.

B. Hard Dense Loop resummation of the gluon propagator.

A Fermi sea of quarks is highly polarizable in an external gauge field and it in turn screens the strength of the external field. This is how the infrared divergence of QCD is

regulated at high baryon density and the effect is included in the hard dense loop (HDL) resummed gluon propagator, which takes the form $\mathcal{D}_{\mu\nu}^{ab}(k, \omega) = \delta^{ab}\mathcal{D}_{\mu\nu}(k, \omega)$ with

$$\mathcal{D}_{ij}^{ab}(\mathbf{k}, \omega) = \frac{-i\delta^{ab}}{k^2 + \omega^2 + \sigma_M(k, \omega)} \left(\delta_{ij} - \frac{k_i k_j}{k^2} \right) \quad (3.15)$$

$$\mathcal{D}_{44}^{ab}(\mathbf{k}, \omega) = \frac{-i\delta^{ab}}{k^2 + \sigma_E(k, \omega)} \quad (3.16)$$

and $\mathcal{D}_{4j}(\mathbf{k}, \omega) = 0$ in Coulomb gauge, where $i\omega$ is the Matsubara energy of the gluon. The ultraviolet divergence has been renormalized. For $k \ll \mu, \omega \ll \mu$, the magnetic self-energy is given by

$$\sigma_M(k, \omega) = m_D^2 f_M\left(\frac{\omega}{k}\right) \quad (3.17)$$

and the electric one by

$$\sigma_E(k, \omega) = m_D^2 f_E\left(\frac{\omega}{k}\right) \quad (3.18)$$

with

$$f_M(z) = \frac{z}{2} \left[(1 + z^2) \tan^{-1} \frac{1}{z} - z \right] \leq \frac{\pi}{4} |z|, \quad (3.19)$$

$$f_E(z) = 1 - z \tan^{-1} \frac{1}{z} \leq 1 \quad (3.20)$$

and

$$m_D^2 = \frac{N_f g^2}{\pi^2} \int_0^\infty dq q \frac{1}{e^{\beta(p-\mu)} + 1} \simeq \frac{N_f g^2 \mu^2}{2\pi^2} \quad (3.21)$$

the Debye mass. As we shall see in the next subsection, the pairing region of energy and momentum, $\omega \ll k$ saturates the upper bound of $f_M(z)$ and $f_E(z)$, and we have effectively

$$\sigma_M(k, \omega) \simeq \frac{\pi}{4} m_D^2 \frac{|\omega|}{k} \quad (3.22)$$

and

$$\sigma_E(k, \omega) \simeq m_D^2 \quad (3.23)$$

The lack of screening in the static limit, $\omega = 0$ gives rise to the forward singularity discussed below.

The HDL resummed gluon propagator in the covariant gauge takes the form

$$\mathcal{D}_{\mu\nu}(\vec{k}, \omega) = \frac{-i}{K^2 + \sigma_M(k, \omega)} P_{\mu\nu}^T - \frac{ik^2}{K^2 [k^2 + \sigma_E(k, \omega)]} P_{\mu\nu}^L - i\xi \frac{K_\mu K_\nu}{(K^2)^2} \quad (3.24)$$

where $P_{ij}^T \equiv \delta_{ij} - \hat{k}_i \hat{k}_j$, $P_{i4}^T = P_{4j}^T = P_{44}^T = 0$, $P_{\mu\nu}^L = \delta_{\mu\nu} - \frac{K_\mu K_\nu}{K^2} - P_{\mu\nu}^T$, $K^2 = k^2 + \omega^2$ and ξ is the gauge parameter.

C. Forward singularity and the leading order contribution.

For the one gluon exchange of Fig. 2, incorporating hard dense loops in the gluon propagator, we find the s -wave amplitudes of the scattering between two quarks of positive energy states

$$\begin{aligned}\tilde{\gamma}_{++++}^{J=0}(\nu', p' | \nu, p) &= -\frac{g^2}{8} \left(1 + \frac{1}{N}\right) \int_{-1}^1 d(\cos \theta) \\ &\times \left[\frac{3 - \cos \theta - (1 + \cos \theta) \frac{(p - p')^2}{|\vec{p} - \vec{p}'|^2}}{(\nu - \nu')^2 + |\vec{p} - \vec{p}'|^2 + m_D^2 f_M \left(\frac{|\nu' - \nu|}{|\vec{p}' - \vec{p}|} \right)} + \frac{1 + \cos \theta}{|\vec{p} - \vec{p}'|^2 + m_D^2 f_E \left(\frac{|\nu' - \nu|}{|\vec{p}' - \vec{p}|} \right)} \right],\end{aligned}\quad (3.25)$$

In the static limit, $\nu = \nu'$, and $p' = p$, the first term of the integrand, the color magnetic interaction becomes singular in the forward direction, and the integral diverges logarithmically in the limit $\frac{|\nu' - \nu|}{|\vec{p}' - \vec{p}|} \rightarrow 0$. If this is the dominant pairing force, we expect that $\nu \sim \nu' \sim k_B T_c$ and the main contribution to the integral comes from the region where

$$|\vec{p}' - \vec{p}|^3 \sim \frac{\pi}{4} m_D^2 |\nu' - \nu| \quad (3.26)$$

The phase space of pairing is restricted to the vicinity of the Fermi surface with $|p' - p| \sim k_B T_c$. Anticipating $\frac{k_B T_c}{\mu} \sim e^{-\frac{\kappa}{g}}$, we have

$$\theta \sim g^{-\frac{2}{3}} \left(\frac{k_B T_c}{\mu} \right)^{\frac{2}{3}} \quad (3.27)$$

and

$$\frac{(p' - p)^2}{(\vec{p}' - \vec{p})^2} \ll 1. \quad (3.28)$$

The integration (3.25) can be approximated by

$$\tilde{\gamma}_{++++}^{J=0}(\nu', p' | \nu, p) \simeq -\frac{g^2}{12 p p'} \left(1 + \frac{1}{N}\right) \log \frac{1}{|\hat{\nu} - \hat{\nu}'|}, \quad (3.29)$$

for $\nu' \sim \nu \sim k_B T_c$, where

$$\hat{\nu} = \left(\frac{N_f}{2} \right)^{\frac{5}{2}} \frac{g^5 \nu}{256 \pi^4 \mu},$$

In terms of the bare quark propagator

$$S_{s',s}(p, \nu) = \frac{i \delta_{s',s}}{i \nu - sp + \mu}, \quad (3.30)$$

the kernel of the Dyson-Schwinger equation reads

$$K_{++++}^{J=0}(\nu', p' | \nu, p) = \frac{g^2}{24 \pi^2} \left(1 + \frac{1}{N_c}\right) \frac{p}{p'} \frac{\log \frac{1}{|\hat{\nu}' - \hat{\nu}|}}{\nu + (p - \mu)^2}. \quad (3.31)$$

The contribution from the states below Dirac sea, being far below the Fermi level, will be suppressed by two powers of $\frac{k_B T}{\mu}$ and will not be considered in this lecture. Accordingly, the s -subscripts which label the states above or below the Dirac sea will be suppressed in the subsequent discussions.

The quark propagators in the kernel $K^{J=0}$ makes the integration over p and the summation over ν logarithmically enhanced for $k_B T \ll \mu$. If the pairing force were free from the forward singularity, this would be the only source of the logarithm. The powers of the logarithm would not grow with the ascending powers of g in the expansion (3.10). The scaling behavior $k_B T_c = c \exp\left(-\frac{\kappa'}{g^2}\right)$ is expected. The exponent (leading term) and the pre-exponential factor (the sub-leading term) can be fixed by carrying out the expansion (3.10) to the second power of the kernel. The forward singularity, however, introduces another logarithm pertaining to the pairing force and its power will grow with that of g . Consequently, the non BCS scaling (2.8) is expected. All terms of the expansion (3.10) have to be retained and the determination of the exponent and the prefactor of (2.8) becomes non-trivial.

To make the integral equation (3.8) tractable, the following approximations are made:

1). A cutoff ν_0 with $k_B T_c \ll \nu_0 \ll \mu$ is introduced for the Matsubara energy and the vertex function (3.25) is replaced by

$$\tilde{\gamma}^{J=0}(\nu', p' | \nu, p) \simeq -\frac{g^2}{12pp'} \left(1 + \frac{1}{N}\right) \log \frac{1}{|\hat{\nu}' - \hat{\nu}|} \theta(\nu_0 - |\nu'|) \theta(\nu_0 - |\nu|), \quad (3.32)$$

2). The logarithm in (3.32) is approximated by

$$\ln \frac{1}{|\hat{\nu}' - \hat{\nu}|} \simeq \ln \frac{1}{|\hat{\nu}_>|} \quad (3.33)$$

with $|\hat{\nu}_>| = \max(|\hat{\nu}'|, |\hat{\nu}|)$ [8].

3). The summation over discrete Matsubara energies is replaced by an integral over continuous Euclidean energy with an infrared cutoff, i.e.

$$\frac{1}{\beta} \sum_{\nu} (\dots) \simeq \int_{|\nu| > \pi k_B T} \frac{d\nu}{2\pi} (\dots) \quad (3.34)$$

The integral equation (3.8) under these approximation becomes separable with respect to the variable p and can be reduced to that with one variable, ν , in terms of the ansatz

$$f(\nu, p) = \frac{1}{p} \phi(\nu) \theta(\nu_0 - |\nu|) \quad (3.35)$$

and we have

$$\phi(x) = k^2 \int_a^b dx' \min(x, x') \phi(x') \quad (3.36)$$

where

$$k^2 = \frac{g^2}{24\pi^2 E} \left(1 + \frac{1}{N_c}\right), \quad (3.37)$$

$a = \ln \frac{1}{\delta}$, $b = \ln \frac{1}{\epsilon}$, and $x = \ln \frac{1}{\nu}$ with

$$\epsilon = \left(\frac{N_f}{2}\right)^{\frac{5}{2}} \frac{g^5 k_B T}{256\pi^3 \mu}, \quad (3.38)$$

and

$$\delta = \left(\frac{N_f}{2}\right)^{\frac{5}{2}} \frac{g^5 \nu_0}{256\pi^4 \mu}. \quad (3.39)$$

Notice that the kernel is symmetric with respect to ν and $-\nu$ and only even functions $\phi(-\nu) = \phi(\nu)$ are considered. The odd functions which vanishes at $\nu = 0$ will not contribute to pairing since $\phi(0) = 0$.

Differentiating both sides of (3.36) twice with respect to x , it is reduced to a differential equation with trigonometric solutions, i.e.

$$\frac{d^2\phi}{dx^2} + k^2\phi = 0. \quad (3.40)$$

Substituting the general solution

$$\phi(x) = A \cos kx + B \sin kx$$

back to the integral equation (3.36), we find the secular equation for the eigenvalues

$$ka \sin k(b-a) = \cos k(b-a) \quad (3.41)$$

with the solution

$$E_j = \frac{g^2(N_c+1)}{6\pi^4(2j+1)^2N_c} \left(\ln \frac{1}{\epsilon}\right)^2 \left[1 + \frac{2}{3}[(j+\frac{1}{2})\pi]^2 \left(\frac{\ln \delta}{\ln \frac{1}{\epsilon}}\right)^3 + O\left(\frac{\ln \delta}{\ln \frac{1}{\epsilon}}\right)^5 \right], \quad (3.42)$$

where $j = 0, 1, 2, \dots$. The corresponding eigenfunction reads

$$\phi_j(x) = \sqrt{\frac{2}{\ln \frac{1}{\epsilon}}} \cos k_j(x-b) \quad (3.43)$$

which satisfies the orthonormal condition

$$\int_a^b dx \phi_i(x) \phi_j(x) = \delta_{ij}. \quad (3.44)$$

The pairing temperature is determined by the condition that the largest eigenvalue, E_0 , crosses one and we obtain that

$$\ln \frac{\mu}{k_B T_{\text{pair}}} = \frac{\kappa}{g} + 5 \ln g - \ln(1024\sqrt{2}N_f^{-\frac{5}{2}}) \quad (3.45)$$

which fixes the leading order term, the non-BCS exponent of (2.8), together with a part of the sub-leading contributions of the perturbation series (3.1).

In appendix B, we shall derive the same eigenvalue condition (3.41) by summing up the perturbative expansion (3.10) of the Fredholm determinant for the equation (3.36).

D. Higher order corrections

It follows from (3.42) and the condition $E_0 = 1$ at $T = T_{\text{pair}}$ that

$$\ln \frac{\mu}{k_B T} \sim \frac{1}{g} \quad (3.46)$$

for the temperature around T_{pair} . Therefore the order of the perturbation series (3.1) does not follows the explicit orders of the kernel diagrams. On the other hand, the forward singularity is not expected to be enhanced in higher order diagrams (an example will be given in the next section). The higher order kernel diagrams are not expected to contribute to the leading order term. In this subsection, we shall develop the systematics to handle the higher order corrections.

To begin with, we construct a complete set of state vectors that diagonalizes the kernel (3.9) to the leading order with discrete Matsubara energies. We introduce

$$\begin{aligned} <\nu, p|0> &= C_0 f_0(\nu, p) \\ <\nu, p|j \neq 0> &= C_j f_j(\nu, p), \end{aligned} \quad (3.47)$$

and $<\nu, p|\alpha>$ with the adjoint expression

$$<|\nu, p>\equiv \frac{<\nu, p|>}{\nu^2 + (p - \mu)^2}, \quad (3.48)$$

where $f_0(\nu, p)$ is given by (3.35) with ϕ exactly ϕ_0 of (3.43) and $f_j(\nu, p)$ ($j \neq 0$) by the same ansatz (3.35) but with ϕ slightly rotated from ϕ_j (3.43) to adapt to the ortho-normal condition with respect to discrete Matsubara energies.

$$< i|j >\equiv \frac{1}{\beta} \sum_{\nu} \int_0^{\infty} dp < i|\nu, p ><\nu, p|j > = \delta_{ij}. \quad (3.49)$$

The complementary set of states, $|\alpha>$ is chosen such that $< j|\alpha > = 0$ and

$$<\alpha'|\alpha> = \delta_{\alpha'\alpha}. \quad (3.50)$$

which together with $|j>$'s make up a complete set of basis, i.e.

$$\sum_j |j><j| + \sum_{\alpha} |\alpha><\alpha| = 1 \quad (3.51)$$

A clear cut zeroth order kernel operator is defined by

$$K_0 = \sum_j E_j^{(0)} |j><j| \quad (3.52)$$

with

$$E_j^{(0)} = \frac{g^2(N_c + 1)}{6\pi^4(2j + 1)^2N_c} \left(\ln \frac{1}{\epsilon} \right)^2. \quad (3.53)$$

The contents of ΔK	The contribution to b
discrete ν vs. continuous ν	$\gamma + \ln 2$
correction to the approximation (3.33)	none
restoring exact σ_M	none
restoring exact σ_E	none
cutoff δ	none
states below Dirac sea	none
higher order kernel diagrams	$-\frac{1}{16}(\pi^2 + 4)(N_c - 1)$

TABLE I. The contributions to the sub-leading term of (3.1)

We have then $K_0|j\rangle = E_j|j\rangle$ and $K_0|\alpha\rangle = 0$. The difference between the exact kernel K and K_0 ,

$$\Delta K \equiv K - K_0 \quad (3.54)$$

generates the perturbation series of the eigenvalue, i.e.

$$E_j = E_j^{(0)} + \langle j|\Delta K|j\rangle + \sum_{i \neq j} \frac{\langle j|\Delta K|i\rangle \langle i|\Delta K|j\rangle}{E_j^{(0)} - E_i^{(0)}} \quad (3.55)$$

$$+ \sum_{\alpha} \frac{\langle j|\Delta K|\alpha\rangle \langle \alpha|\Delta K|j\rangle}{E_j^{(0)}} + \dots,$$

and the transition temperature is determined by $E_0 = 1$.

The analysis of perturbative corrections to the sub-leading order is rather laborious. We find few contributions from the first order term of (3.55) and none from the second order terms. Except for the contribution from the quark self-energy to be discussed in the next section, the details of the analysis will not be presented here. The interested reader is referred to the original work [15]. The result of the analysis is shown in Table I.

A similar perturbation theory has been developed for the energy gap below T_c [33].

E. Pairing at a nonzero angular momentum

For equal helicity pairing, there is no net spin projection in the direction of the relative spatial momentum of the pairing quarks. The total angular momentum $J \geq 0$ and the corresponding angular wave function is the Legendre polynomial, $P_J(\cos \theta)$. The partial wave component of the one-gluon exchange vertex is given by [15]

$$\tilde{\gamma}^J(\nu', p' | \nu, p) = -\frac{g^2}{8} \left(1 + \frac{1}{N}\right) \int_{-1}^1 d(\cos \theta) P_J(\cos \theta) \quad (3.56)$$

$$\times \left[\frac{3 - \cos \theta - (1 + \cos \theta) \frac{(p - p')^2}{|\vec{p} - \vec{p}'|^2}}{(\nu - \nu')^2 + |\vec{p} - \vec{p}'|^2 + m_D^2 f_M \left(\frac{|\nu' - \nu|}{|\vec{p}' - \vec{p}|} \right)} + \frac{1 + \cos \theta}{|\vec{p} - \vec{p}'|^2 + m_D^2 f_E \left(\frac{|\nu' - \nu|}{|\vec{p}' - \vec{p}|} \right)} \right].$$

It follows from the forward singularity and the fact that $P_J(1) = 1$ that the leading order contribution should be independent of J . To figure J -dependence in the sub-leading order, we write

$$P_J(\cos \theta) = 1 + [P_J(\cos \theta) - 1] \quad (3.57)$$

and correspondingly

$$\tilde{\gamma}^J(\nu', p' | \nu, p) = \tilde{\gamma}^{J=0}(\nu', p' | \nu, p) - \frac{g^2}{2\mu^2} \left(1 + \frac{1}{N_c}\right) s_J \quad (3.58)$$

Since the expression inside the bracket of (3.57) smears the forward singularity, the HDL self energies, σ_M and σ_E , can be dropped and the momenta p, p' can be set at μ when evaluating s_J . We find that

$$s_J = \frac{1}{2} \int_{-1}^1 d \cos \theta \frac{P_J(\cos \theta) - 1}{1 - \cos \theta}. \quad (3.59)$$

Using the recursion formula for Legendre polynomials,

$$(J+1)P_{J+1}(\cos \theta) - (2J+1)\cos \theta P_J(\cos \theta) + JP_{J-1}(\cos \theta) = 0, \quad (3.60)$$

we find that,

$$(J+1)s_{J+1} - (2J+1)s_J + Js_{J-1} = -\delta_{J0}. \quad (3.61)$$

Since $c_0 = 0$, the solution to (3.61) for $J \geq 1$ is,

$$s_J = - \sum_{n=1}^J \frac{1}{n}. \quad (3.62)$$

For a cross helicity pairing, the spin projection in the direction of the relative momentum of the pairing quarks is one and the total angular momentum $J \geq 1$ (the orbital angular momentum is always perpendicular to the relative momentum). The corresponding angular wave function is the Wigner D -function $d_{11}^J(\theta)$ defined by

$$d_{M'M}^J(\theta) = \langle JM' | e^{-iJ_y\theta} | JM \rangle \quad (3.63)$$

and the corresponding partial wave component of the vertex function reads [15]

$$\begin{aligned} \tilde{\gamma}'^J(\nu', p' | \nu, p) &= -\frac{g^2}{8} \left(1 + \frac{1}{N}\right) (2J+1) \int_{-1}^1 d(\cos \theta) d_{11}^J(\theta) \\ &\times \left[\frac{1 + \cos \theta - (1 + \cos \theta) \frac{(\vec{p} - \vec{p}')^2}{|\vec{p} - \vec{p}'|^2}}{(\nu - \nu')^2 + |\vec{p} - \vec{p}'|^2 + m_D^2 f_M \left(\frac{|\nu' - \nu|}{|\vec{p}' - \vec{p}|} \right)} + \frac{1 + \cos \theta}{|\vec{p} - \vec{p}'|^2 + m_D^2 f_E(x)} \right]. \\ &= \tilde{\gamma}^{J=0}(\nu', p' | \nu, p) - \frac{g^2}{2\mu^2} \left(1 + \frac{1}{N_c}\right) s'_J \end{aligned} \quad (3.64)$$

Following the same strategy for equal helicity pairing, we find that



FIG. 5. The quark self-energy diagram.

$$\begin{aligned}
 s'_J &= \frac{1}{2} \int_{-1}^1 d \cos \theta \frac{d_{11}^J(\theta) \cos^2 \frac{\theta}{2} - 1}{1 - \cos \theta} \\
 &= \frac{1}{2} \left(s_J + \frac{J}{2J+1} s_{J+1} + \frac{J+1}{2J+1} s_{J-1} \right).
 \end{aligned} \tag{3.65}$$

The leading order degeneracy among different angular momentum makes pairing vulnerable to distortion in the presence of an anisotropic perturbation. This will impact on the LOFF pairing to be discussed in section V.

IV. THE HIGHER ORDER KERNEL DIAGRAMS.

A. The quark self-energy function

Another important consequence of the forward singularity is the non Fermi liquid behavior of the quark self energy, which has been considered in solid state physics in the context of electrodynamics with quarks replaced by electrons and gluons by photons [32]. The kinks of the single particle occupation number distribution function at Fermi surface and $T = 0$ is smeared and the electronic specific heat acquires a term proportional to $T \ln T$ at low T . Both effects are too small to be observed in a nonrelativistic system. For an ultra relativistic system like the dense quark matter considered here, the impact is large and will lower the color superconductivity scales significantly because of the suppressed quasi-particle weight towards the Fermi surface. The quark self energy function $\Sigma(P)$ is represented by Fig. 5, with the gluon line containing HDL resummation. Standard Feynman rules yield

$$\Sigma(P) = C_f \Xi(P) \tag{4.1}$$

with $C_f = T_f^l T_f^l = \frac{N_c^2 - 1}{2N_c}$ for T_f in the fundamental representation of $SU(N_c)$ and

$$\Xi(P) = -\frac{g^2}{\beta} \sum_{\omega} \int \frac{d^3 \vec{l}}{(2\pi)^3} \mathcal{D}_{\mu\nu}(L) \gamma_{\mu} S(L + P) \gamma_{\nu}, \tag{4.2}$$

where $L = (\vec{l}, -\omega)$, $P = (\vec{p}, -\nu)$ with ω and ν the Masubara energy of the internal gluon and quark propagators. The bare quark propagator is given by

$$S(P) = \frac{i}{\not{P}}, \tag{4.3}$$

with $\not{P} \equiv \gamma_4(\mu + i\nu) - i\vec{\gamma} \cdot \vec{p}$. All gamma matrices are hermitian. Introduce the infrared sensitive region of the loop energy-momentum, $0 < l < l_c$ and $-\omega_c < \omega < \omega_c$ with $l_c, \omega \ll \mu$, we have

$$\Xi(P) = \Xi^<(P) + \Xi^>(P) \quad (4.4)$$

with the superfixes denoting the integration inside and outside the infrared sensitive region and we shall evaluate $\Xi^<(P)$ only.

$$\begin{aligned} \Xi^<(P) &\simeq -\frac{g^2}{4\pi^2} \int_0^{l_c} dl l^2 \int_{-1}^1 d(\cos\theta) \frac{1}{\beta} \sum_{|\omega|<\omega_c} \frac{\gamma_4 - i(\hat{l} \cdot \hat{p})^2 \vec{\gamma} \cdot \hat{p}}{\xi - i(\omega + \nu)} \mathcal{D}(l, \omega_n) \\ &\simeq -\frac{g^2}{8\pi^3} \int_0^{l_c} dl l \int_{-\omega_c}^{\omega_c} d\omega \mathcal{D}(l, \omega) F(\nu, p; l, \omega), \end{aligned} \quad (4.5)$$

where

$$F(\nu, p; l, \omega) = \int_{p-\mu-l}^{p-\mu+l} d\xi \frac{1 - \frac{\mu^2}{l^2 p^2} (\xi - p + \mu)^2}{\xi - i(\omega + \nu)}. \quad (4.6)$$

Carrying out the integral for $p = \mu$, we obtain that

$$F(\nu, \mu; l, \omega) = 2i\gamma_4 \tan^{-1} \frac{l}{\omega + \nu} + 2\frac{\omega + \nu}{l} \vec{\gamma} \cdot \hat{p} \left(1 - \frac{\omega + \nu}{l} \tan^{-1} \frac{l}{\omega + \nu} \right) \quad (4.7)$$

and

$$\begin{aligned} \frac{\partial}{\partial \nu} F(\nu, \mu; l, \omega) &= 2\pi i \gamma_4 \delta(\nu + \omega) - \frac{2il}{(\omega + \nu)^2 + l^2} \gamma_4 \\ &\quad + \frac{2}{l} \left[-2\frac{\omega + \nu}{l} \tan^{-1} \frac{l}{\omega + \nu} + \frac{2(\omega + \nu)^2 + l^2}{(\omega + \nu)^2 + l^2} \right] \vec{\gamma} \cdot \hat{p}, \end{aligned} \quad (4.8)$$

where the delta function comes from the discontinuity of the inverse tangent function. We find the energy dependence of the self-energy by differentiating,

$$\frac{\partial}{\partial \nu} \Xi^<(\nu, \vec{p}) \Big|_{p=\mu} = g^2 [A(\nu) + B(\nu)], \quad (4.9)$$

with

$$A(\nu) = \frac{-i}{4\pi^2} \gamma_4 \int_0^{l_c} dl \frac{l}{l^2 + \nu^2 + m_D^2 f_M \left(\frac{-\nu}{l} \right)} \quad (4.10)$$

and

$$\begin{aligned} B(\nu) &= \frac{i}{2\pi^3} \int_0^{l_c} dl \int_{-\omega_c}^{\omega_c} d\omega \mathcal{D}(l, \omega) \left\{ \frac{il}{(\omega + \nu)^2 + l^2} \gamma_4 \right. \\ &\quad \left. - \frac{1}{l} \left[-2\frac{\omega + \nu}{l} \tan^{-1} \frac{l}{\omega + \nu} + \frac{2(\omega + \nu)^2 + l^2}{(\omega + \nu)^2 + l^2} \right] \vec{\gamma} \cdot \hat{p} \right\} \end{aligned} \quad (4.11)$$

Noting that the asymptotic behavior, that $f_M(z) \sim |z|$ for $|z| \ll 1$, a scale l_0 may be introduced to divide the integration in $A(\nu)$ further into two: $|\nu| \ll l_0 \ll (m_D^2 |\nu|)^{1/3}$. For $l < l_0$ we have the contribution

$$\int_0^{l_0} dl \frac{l}{l^2 + \nu^2 + m_D^2 f_M\left(\frac{\nu}{l}\right)} \leq \frac{1}{m_D^2} \int_0^{l_0} dl \frac{l}{f_M\left(\frac{\nu}{l}\right)} < \frac{1}{m_D^2 f_M\left(\frac{\nu}{l}\right)} \int_0^{l_0} dl l \simeq \frac{l_0^3}{m_D^2 |\nu|} \ll 1. \quad (4.12)$$

All of the inequalities follows straightforwardly from the definition of l_0 except for the second, which is because of $f_M(\nu/l)$ being a monotonically decreasing function of l . Neglecting this sub-leading contribution, we find an infrared logarithm in $A(\nu)$ arising from the second region (namely the region $l_0 < l < l_c$). The integration $B(\nu)$ is, however, finite in the limit $\nu \rightarrow 0$. We end up with

$$\frac{\partial}{\partial \nu} \Xi^<(\nu, p) = -\frac{i}{4\pi^2} \int_{l_0}^{l_c} dl \frac{l^2}{l^3 + \nu^2 l + m_D^2 |\nu|} \simeq -\frac{ig^2}{12\pi^2} \gamma_4 \ln \frac{4l_c^3}{\pi m_D^2 |\nu|} \quad (4.13)$$

and

$$\frac{\partial}{\partial p} \Xi^<(\nu, p) = ig^2 B(\nu) = \text{finite} \quad (4.14)$$

at $p = \mu$. It follows then that

$$\Sigma(P) |_{p=\mu} = -\frac{ig^2}{12\pi^2} C_f \gamma_4 \nu \ln \frac{4l_c^3}{\pi m_D^2 |\nu|} + \dots \quad (4.15)$$

B. The contribution of the quark self-energy to the sub-leading term

Because of the trade off (3.46), the quark self-energy represents a order g correction to the leading order kernel diagrams and therefore contributes to the sub-leading term of (3.1). The calculation of this contribution proceeds as follows [14]:

The quark propagator with the self-energy correction reads

$$\mathcal{S}(p, \nu) = \frac{i}{i\nu - p + \mu} + \Delta S(p, \nu) \quad (4.16)$$

where

$$\Delta S(p, \nu) = \frac{i}{(i\nu - p + \mu)^2} \Sigma(p, \nu) \quad (4.17)$$

with

$$\Sigma(p, \nu) = \bar{u}(\vec{p}) \Sigma(P) u(\vec{p}) = -\frac{ig^2}{12\pi^2} C_f \nu \ln \frac{4l_c^3}{\pi m_D^2 |\nu|}. \quad (4.18)$$

The corresponding correction to the kernel is

$$\Delta K(\nu', p' | \nu, p) = \frac{p^2}{2\pi^2} \tilde{\gamma}^J(\nu', p' | \nu, p) [\Delta S(p, \nu) S(p, -\nu) + S(p, \nu) \Delta S(p, -\nu)] \quad (4.19)$$

Applying the perturbation theory developed in the previous section, we find the first order shift of the maximum eigenvalue of the Fredholm kernel [14]

$$\begin{aligned}
\delta E_0 &= \frac{1}{\beta^2} \sum_{\nu'} \sum_{\nu} \int_0^\infty dp' \int_0^\infty dp \bar{f}_0(\nu', p') \Delta K(\nu', p' | \nu, p) f_0(\nu, p) \\
&\simeq -E_0^{(0)} \int_{\pi k_B T}^\delta \frac{d\nu}{\pi} \int_0^\infty dp p^2 f_0^J(\nu, p) [\Delta S(p, \nu) S(p, -\nu) + S(p, \nu) \Delta S(p, -\nu)] f_0^J(\nu, p) \\
&\simeq -E_0^{(0)} \frac{N_c^2 - 1}{N_c} \frac{g^2}{12\pi^2} \int_{\pi k_B T}^\delta \frac{d\nu}{\pi} \nu^2 \phi^2(\nu) \ln \frac{4l_c^3}{\pi m_D^2 |\nu|} \int_0^\infty dp \frac{1}{[\nu^2 - (p - \mu)^2]^2} \\
&\simeq -E_0^{(0)} \frac{N_c^2 - 1}{N_c} \frac{g^2}{3\pi^4} \ln \frac{1}{\epsilon} \int_0^{\frac{\pi}{2}} dx x \sin^2 x \\
&\simeq -\frac{g^2}{48\pi^4} \frac{N_c^2 - 1}{N_c} (\pi^2 + 4) E_0^{(0)} \ln \frac{1}{\epsilon},
\end{aligned} \tag{4.20}$$

where the wave function $f_0^J(\nu, p)$ is given by the ansatz (3.35) with ϕ_0 by (3.43). Upon setting the corrected maximum eigenvalue,

$$E_0 = \frac{g^2}{6\pi^4} \frac{N_c + 1}{N_c} \left[\ln^2 \frac{1}{\epsilon} + 2(\gamma + \ln 2 + 6s_J) \ln \frac{1}{\epsilon} - \frac{g^2}{48\pi^4} \frac{N_c^2 - 1}{N_c} (\pi^4 + 4) \ln^3 \frac{1}{\epsilon} \right], \tag{4.21}$$

to one, we end up with

$$\ln \frac{1}{\epsilon} = \sqrt{\frac{6N_c}{N_c + 1}} \frac{\pi^2}{g} - \gamma - \ln 2 + 6s_J + \frac{N_c - 1}{16} (\pi^2 + 4). \tag{4.22}$$

According to the arguments given in the rest of this section, we have completed the sub-leading term of (3.1) and the scaling formula of the pairing temperature (2.8) follows from (4.22).

C. The infrared behavior of the vertex functions.

The contribution of the quark self energy to the sub-leading term of the perturbation series (3.1) raises naturally the issues of the contribution from the vertex corrections, since they are intimately related through BRST identity of the nonAbelian gauge invariance. On the other hand, the Fermi sea makes the infrared behavior of the vertex function to depend subtly on the order of the infrared limit, i.e. the limit of zero energy transfer and zero momentum transfer. Consequently, we find that the contribution from the vertex correction is beyond the sub-leading order without contradicting to the BRST identity. In this subsection we shall explore the infrared behavior of the vertex correction and demonstrate the absence of its contribution to the sub-leading terms of (3.1). The matching of the BRST identity to the leading infrared logarithm will be discussed in the next subsection.

The vertex corrections are listed in Fig. 6. We begin with the first of them, which presents in an abelian gauge theory, say QED, as well. In order to simplify matters further, we shall put the spatial momenta of both external quarks on the Fermi surface, i.e. $p = p' = \mu$. We have

$$\Lambda_\mu^{l(a)}(P', P) = g T_f^m T_f^l T_f^m \Lambda_\mu(P', P) = g T_f^l \left(-\frac{C_{ad}}{2} + C_f \right) \Lambda_\mu(P', P), \tag{4.23}$$

where

$$\Lambda_\mu(P', P) = \frac{i}{\beta} g^2 \sum_\omega \int \frac{d^3 \vec{l}}{(2\pi)^3} \mathcal{D}_{\nu\rho}(\vec{l}, \omega) \gamma_\nu S(L + P') \gamma_\mu S(L + P) \gamma_\rho, \quad (4.24)$$

and $C_a d\delta^{c'c} = f^{abc'} f^{abc} = N_c \delta^{c'c}$. This may be written in terms of two integrals, one inside and one outside the infra-red sensitive region: $0 < l < l_c$, $-\omega_c < \omega < \omega_c$ with $l_c, \omega_c \ll \mu$,

$$\Lambda_\mu(P', P) = \hat{P}_\mu \left[\Lambda^{(a)<}(P', P) + \Lambda^{(a)>}(P', P) \right]. \quad (4.25)$$

with $\hat{P} = (-i\hat{p}, 1)$. As we are only interested in the leading infra-red behavior, we evaluate $\Lambda^{(a)<}(P', P)$ only,

$$\Lambda^{(a)<}(P', P) \simeq \frac{g^2}{8\pi^3} \int_0^{l_c} dl l^2 \int_{-1}^1 d(\cos\theta) (\gamma_4 - i\vec{\gamma} \cdot \hat{p} \cos^2\theta) \tilde{\Lambda}(P, P'; L) \sin^2\theta, \quad (4.26)$$

$$\tilde{\Lambda}(P, P'; L) = \oint \frac{d\omega}{2\pi} \frac{\mathcal{D}(l, \omega)}{\zeta' - \zeta} \left(\frac{1}{\omega + \zeta'} - \frac{1}{\omega - \zeta'} - \frac{1}{\omega + \zeta} + \frac{1}{\omega - \zeta} \right) \ln(-\omega), \quad (4.27)$$

where $\zeta = \nu + i\xi$, $\xi = |\vec{l} + \vec{p}| - \mu$ and ζ' and ξ' refer to ν' , \vec{p}' . The logarithm in (4.27) introduces a branch cut which we may take to lie along the positive real axis and the contour to run above and below it in the normal fashion. As shown for the self-energy, it is only the discontinuities that occur as poles cut the contour and branch cut that induce the infra-red singularity. Hence we need only focus upon the second and fourth terms in (4.27), since the other terms are regular. Using the convention that $\arg(-\omega) = 0$ along the negative real axis, we find that the contribution of these poles reads

$$\tilde{\Lambda}_{\text{disc.}}(P', P; L) = \frac{\pi}{\zeta' - \zeta} [\text{Sign}(\xi) \mathcal{D}(l, \zeta) - \text{Sign}(\xi') \mathcal{D}(l, \zeta')], \quad (4.28)$$

where the sign function comes from the discontinuity of $\ln(-\omega)$ crossing the cut.

We are now in a position to examine the limit $P_\mu \rightarrow P'_\mu$ and we shall consider the two different orderings of the limits in turn:

$$i) \quad \lim_{\nu' \rightarrow \nu} \lim_{\vec{p}' \rightarrow \vec{p}} \tilde{\Lambda}_{\text{disc.}}(P', P; L) = -\pi \text{Sign}(\xi) \frac{\partial}{\partial \nu} \mathcal{D}(l, \zeta), \quad (4.29)$$

$$ii) \quad \lim_{\vec{p}' \rightarrow \vec{p}} \lim_{\nu' \rightarrow \nu} \tilde{\Lambda}_{\text{disc.}}(P', P; L) = i\pi \frac{\partial}{\partial \xi} [\text{Sign}(\xi) \mathcal{D}(l, \zeta)]. \quad (4.30)$$

In both cases we are looking at the infra-red limit, and thus fix the external momentum to be $p = p' = \mu$.

First of all, considering case *i*), changing the integration variable from $d\cos\theta$ to $d\xi$, it is straightforward to find,

$$\lim_{\nu' \rightarrow \nu} \lim_{\vec{p}' \rightarrow \vec{p}} \Lambda^{(a)<}(P', P) \Big|_{p=\mu} = -\frac{g^2}{8\pi^2} \int_0^{l_c} dl l \int_{-l}^l d\xi \text{Sign}(\xi) \frac{\partial}{\partial \nu} \mathcal{D}(l, \zeta) \left(\gamma_4 - i\frac{\xi^2}{l^2} \vec{\gamma} \cdot \hat{p} \right) \quad (4.31)$$

$$\begin{aligned} &= \frac{ig^2}{4\pi^2} \gamma_4 \int_0^{l_c} dl l [\mathcal{D}(l, \nu) - \mathcal{D}(l, \nu + il)] \\ &= \frac{ig^2}{12\pi^2} \gamma_4 \ln \frac{4l_c^3}{\pi m_D^2 \nu} + \dots, \end{aligned} \quad (4.32)$$

where the second term inside the brackets of the second line of eq.(4.32) is free from logarithmic divergence in the limit $\nu \rightarrow 0$ and is denoted by ellipses in (4.32).

Secondly, considering case *ii*), we find that differentiation gives two terms which will cancel in the leading order,

$$\lim_{\vec{p}' \rightarrow \vec{p}} \lim_{\nu' \rightarrow \nu} \Lambda^{(a)<} (P', P) \Big|_{p=\mu} = \frac{ig^2}{8\pi^2} \int_0^{l_c} dl l \int_{-l}^l d\xi \left(\gamma_4 - i \frac{\xi^2}{l^2} \vec{\gamma} \cdot \hat{p} \right) \left[\text{Sign}(\xi) \frac{\partial}{\partial \xi} \mathcal{D}(l, \zeta) + 2\delta(\xi) \mathcal{D}(l, \zeta) \right]. \quad (4.33)$$

The first term is identical to that evaluated for case *i*) above. With the same approximation, the second term is,

$$\frac{-i}{4\pi^2} \int_0^{l_c} dl \frac{l^2}{l^3 + m_D^2 \nu} \simeq \frac{-i}{12\pi^2} \ln \frac{l_c^3}{m_D^2 \nu}. \quad (4.34)$$

The leading contributions of the two terms cancel and in this ordering of limits the vertex is free from the infrared logarithm.

When this vertex diagram is inserted in to the kernel of the Dyson-Schwinger equation for di-quark scattering, the important contribution to the pairing, as is determined by the forward singularity of the one gluon exchange, comes from

$$|\vec{p}' - \vec{p}|^3 \sim m_D^2 |\nu' - \nu| \quad (4.35)$$

which means that

$$|\vec{p}' - \vec{p}| \gg |\nu' - \nu| \quad (4.36)$$

according to (3.27) and is away from the region of energy-momentum transfer,

$$|\vec{p}' - \vec{p}| \ll |\nu' - \nu| \quad (4.37)$$

in which the vertex correction is enhanced logarithmically. This is the reason for the absence the absence of the vertex correction from Fig.6a in the sub-leading terms of (3.1) and the statement was also verified numerically [16]. We have also checked explicitly that the vertex correction Fig. 6b does not contribute to the sub-leading term. The absence of the contribution of Fig. 6c to the sub-leading term follows from the BRST identity discussed below.

D. Matching the BRST identity.

In this subsection, we shall show that the absence of the vertex corrections in the sub-leading terms is not in conflict with the BRST identity of the gauge symmetry. The BRST identity is the generalization of the Ward identity of an Abelian gauge theory to a non-Abelian gauge theory and it takes the form for one-loop diagrams incorporating HDL gluon propagators [16]

$$(P' - P)^\mu \Lambda_\mu^l (P', P) = T_f^l (\Sigma(P') - \Sigma(P)) + (P' - P)_\mu R_\mu^l (P', P). \quad (4.38)$$

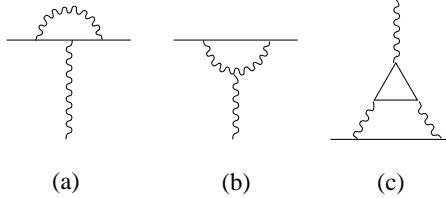


FIG. 6. The physical radiative corrections to the quark-gluon vertex; a) $\Lambda_\mu^{l(a)}$, the abelian vertex, b) $\Lambda_\mu^{l(b)}$, the tri-gluon vertex and c) $\Lambda_\mu^{l(c)}$, the triangular vertex.

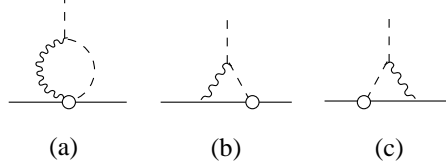


FIG. 7. The non-physical ghost diagrams generated by the BRST transformations; representing a) $R^{l(a)}$, b) $R^{l(b)}$ and c) $R^{l(c)}$.

The physical quark-gluon vertices $\Lambda_\mu^l = \Lambda_\mu^{l(a)} + \Lambda_\mu^{l(b)} + \Lambda_\mu^{l(c)}$ are represented in Fig 6. The non-physical ghost-quark vertices generated by the BRST transformation, $R^l = R^{l(a)} + R^{l(b)} + R^{l(c)}$, are represented in Fig. 7 and vanish for on-shell Minkowski momenta P and P' at $\mu = 0$.

To prove this identity, we start with the Feynman amplitudes of the quark self energy diagram of Fig 5.

$$\Sigma(P) = -C_f \frac{g^2}{\beta} \sum_n \int \frac{d^3 \vec{l}}{(2\pi)^3} \mathcal{D}_{\mu\nu}(L) \gamma_\mu S(P+L) \gamma_\nu. \quad (4.39)$$

and the vertex diagram of Fig 6a.

$$\Lambda_\mu^{l(a)}(P', P) = -T_f^m T_f^l T_f^m \frac{g^3}{\beta} \sum_n \int \frac{d^3 \vec{l}}{(2\pi)^3} \mathcal{D}_{\nu\rho}(\vec{l}, |\omega_n|) \gamma_\nu S(P'+L) \gamma_\mu S(P+L) \gamma_\rho. \quad (4.40)$$

Using the standard trick,

$$(P' - P)^\mu S(P'+L) \gamma_\mu S(P+L) = S(P'+L) - S(P+L), \quad (4.41)$$

we may trivially rewrite this expression in terms of the self-energy,

$$(P' - P)^\mu \Lambda_\mu^{l(a)}(P', P) = T_f^l \left(1 - \frac{C_{ad}}{2C_f} \right) [\Sigma(P') - \Sigma(P)]. \quad (4.42)$$

For QED $C_{ad} = 0$ and (4.42) becomes the ordinary Ward identity. However, for non-abelian gauge theories, the group theoretic factor do not match but we have additional vertices which cancel the extra term.

The Feynman amplitude of the second vertex diagram of Fig. 6 reads

$$\Lambda_\mu^{l(b)}(P', P) = f^{lmn} T_f^m T_f^n \frac{g^3}{\beta} \sum_n \int \frac{d^3 \vec{l}}{(2\pi)^3} \mathcal{D}_{\nu\lambda}(L)(-i)\Gamma_{\mu\lambda\rho}(L, L-Q) \mathcal{D}_{\rho\nu'}(L) \gamma_\nu S(P+L) \gamma_{\nu'}, \quad (4.43)$$

where $if^{lmn} T_f^m T_f^n = -\frac{C_{ad}}{2} T_f^l$ and $\Gamma_{\mu\lambda\rho}(P', P)$ denotes the bare tri-gluon vertex. Using the explicit expression of $\Gamma_{\mu\lambda\rho}(P', P)$ and the Dyson-Schwinger equation for a HDL gluon propagator,

$$\mathcal{D}_{\mu\nu}(K) = D_{\mu\nu}(K) - i\mathcal{D}_{\mu\rho}(K)\Pi_{\rho\lambda}(K)D_{\lambda\nu}(K) \quad (4.44)$$

with $D(K)$ the free gluon propagator. We find that

$$(P' - P)^\mu \mathcal{D}_{\nu'\lambda}(P') \Gamma_{\mu\lambda\rho}(P', P) \mathcal{D}_{\rho\nu}(P) = ig[V_{\nu'\nu}^{(1)}(P', P) + V_{\nu'\nu}^{(2)}(P', P) + V_{\nu'\nu}^{(3)}(P', P)], \quad (4.45)$$

where

$$\begin{aligned} V_{\nu'\nu}^{(1)}(P', P) &= i[\mathcal{D}_{\nu'\nu}(P) - \mathcal{D}_{\nu'\nu}(P')], \\ V_{\nu'\nu}^{(2)}(P', P) &= \mathcal{D}_{\nu'\lambda}(P') [\Pi_{\lambda\rho}(P') - \Pi_{\lambda\rho}(P)] \mathcal{D}_{\rho\nu}(P), \\ V_{\nu'\nu}^{(3)}(P', P) &= \Delta(P') P'_{\nu'} P'_\lambda \mathcal{D}_{\lambda\nu}(P) - \mathcal{D}_{\nu'\lambda}(P') P_\lambda P_\nu \Delta(P). \end{aligned} \quad (4.46)$$

with $\Delta(P) = -\frac{i}{P^2}$ the ghost propagator. Correspondingly, we have

$$(P' - P)^\mu \Lambda_\mu^{l(b)}(P', P) = I_1^l(P', P) + I_2^l(P', P) + I_3^l(P', P) \quad (4.47)$$

with

$$I_j^l(P', P) = \frac{1}{2} C_{ad} g^3 T_f^l \int \frac{d^4 L}{(2\pi)^4} V_{\mu\nu}^{(j)}(L, L - P' + P) \gamma_\nu S(P + L) \gamma_\mu. \quad (4.48)$$

It is straightforward to show that,

$$(P' - P)^\mu \Lambda_\mu^{l(a)}(P', P) + I_1^l(P', P) = g T_f^l [\Sigma(P') - \Sigma(P)] \quad (4.49)$$

and $I_3^l(P', P) = (P' - P)_\mu R_\mu^l(P', P)$. The second term on RHS of (4.47) is to be canceled by the third vertex diagrams, Fig. 6c.

Denoting by $\tilde{\Gamma}_{\mu\lambda\rho}^{lmn}(P', P)$ the triangular vertex in Fig. 8 and using the identity

$$(P' - P)_\mu \tilde{\Gamma}_{\mu\lambda\rho}^{lmn}(P', P) = ig f^{lmn} [\Pi_{\lambda\rho}(P') - \Pi_{\lambda\rho}(P)] \quad (4.50)$$

we find that

$$(P' - P)^\mu \Lambda_\mu^{l(c)}(P', P) + I_2^l(P', P) = 0 \quad (4.51)$$

and the BRST identity (4.38) is established.

As is shown in the previous subsection, the infrared logarithm shows up in the limit $\nu' \rightarrow \nu$ following $\vec{p}' \rightarrow \vec{p}$, i.e.

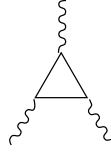


FIG. 8. Quark loop with three external gluons, $\tilde{\Gamma}_{\mu\lambda\rho}^{lmn}$.

$$\lim_{\nu' \rightarrow \nu} \lim_{\vec{p}' \rightarrow \vec{p}} \Lambda_{\mu}^{l(a)}(P', P) = T_f^l \left(-\frac{C_{ad}}{2} + C_f \right) \frac{ig^3}{12\pi^2} \gamma_4 \ln \frac{4l_c^3}{\pi m_D^2 |\nu|}, \quad (4.52)$$

In the same order of limit, the BRST identity becomes

$$\lim_{\nu' \rightarrow \nu} \lim_{\vec{p}' \rightarrow \vec{p}} [\Lambda_4^l(P', P) - R_4^l(P', P)] = -g T_f^l \frac{\partial}{\partial \nu} \Sigma(P). \quad (4.53)$$

It has been shown in [16] that both $\Lambda_4^{l(b)}(P', P)$ and $R_4^l(P', P)$ are free from the infrared logarithm in this limit, but $\Lambda_{\mu}^{l(c)}(P', P)$ contributes one,

$$\lim_{\nu' \rightarrow \nu} \lim_{\vec{p}' \rightarrow \vec{p}} \Lambda_4^{l(c)}(P', P) = i \frac{g^3}{24\pi^2} C_{ad} \gamma_4 T_f^l \ln \frac{4l_c^3}{\pi m_D^2 |\nu|}, \quad (4.54)$$

which together with (4.52) and (4.53) match the leading logarithm of the BRST identity.

The presence of $\Lambda_{\mu}^{l(c)}(P', P)$ in the BRST identity is not surprising in terms of the standard proof of Ward identity by summing up all possible insertions of a gauge boson line into a fermion self energy diagram. Since HDL resummation is employed for gluon propagators, the inserted gluon line may land on one of HDL's and give rise to $\Lambda_{\mu}^{l(c)}$.

It is worth mentioning that the nonzero chemical potential makes the triangle vertex of Fig. 8 non-vanishing for QED as well. But it will not contribute to the Ward identity with HDL photons because the RHS of (4.50) vanishes.

The BRST identity in the superconducting phase is discussed in [19].

E. The crossed box diagram with two gluon exchange.

Now we come to the last 2PI vertex shown in Fig. 4, which contains two HDL gluon lines crossing each other. This was estimated in [8] by a renormalization group argument. The explicit calculation of this diagram in [14] will be outlined below.

Apart from a group theoretic factor, the contribution of the crossed box diagram to $\tilde{\gamma}_{+++}^0$ reads

$$B = -\frac{1}{2} g^4 \int_{-1}^1 d\cos\theta \int_{-\infty}^{\infty} \frac{d\omega}{2\pi} \int \frac{d^3 \vec{l}}{(2\pi)^3} \mathcal{D}_{\mu\mu'}(\vec{l} - \frac{\vec{q}}{2}, \omega) \mathcal{D}_{\nu\nu'}(\vec{l} + \frac{\vec{q}}{2}, \omega) \\ \times [\bar{u}(\vec{p}') \gamma_{\mu} S_F(\vec{P} + \vec{l}, \omega) \gamma_{\nu} u(\vec{p}')] [\bar{u}(-\vec{p}') \gamma_{\nu'} S_F(-\vec{P} + \vec{l}, \omega) \gamma_{\mu'} u(-\vec{p})], \quad (4.55)$$

where $|\vec{p}| = |\vec{p}'| = \mu$, $\vec{P} = \frac{1}{2}(\vec{p} + \vec{p}')$, $\vec{q} = \vec{p} - \vec{p}'$ and the discrete Matsubara energies have been replaced by continuous Euclidean energies with the external ones set to zero. Ignoring

the Coulomb propagator, the contribution from the small scattering angle, $|\theta| < \theta_0 \ll 1$, and the infrared region $|\vec{l}| \ll \mu$, $|\omega| \ll \mu$,

$$B_{\text{IR}} = -\frac{1}{2}g^4 \int_{-\theta_0}^{\theta_0} d\theta \sin \theta \int_{\text{IR}} \frac{d\omega}{2\pi} \frac{d^3 \vec{l}}{(2\pi)^3} \mathcal{D}_{ii'}(\vec{l} - \frac{\vec{q}}{2}, i\omega) \mathcal{D}_{jj'}(\vec{l} + \frac{\vec{q}}{2}, i\omega) \times [\bar{u}(\vec{p}') \gamma_i S_F(\vec{P} + \vec{l}, i\omega) \gamma_j u(\vec{p})] [\bar{u}(-\vec{p}') \gamma_{j'} S_F(-\vec{P} + \vec{l}, i\omega) \gamma_{i'} u(-\vec{p})], \quad (4.56)$$

is bounded: $B_{\text{IR}} \leq I$, where

$$I \equiv \frac{1}{32\pi^4 \mu^2} \int_0^{\theta_0} d\theta \int_{\text{IR}} d\rho d^3 \vec{r} \frac{r_+ r_- |E_+ E_- - \rho^2|}{(r_+^3 + \kappa|\rho|)(r_-^3 + \kappa|\rho|)(\rho^2 + E_+^2)(\rho^2 + E_-^2)}. \quad (4.57)$$

Here $E_{\pm} = |\vec{P} \pm \vec{l}|/\mu - 1$, $r_{\pm} = |\vec{l} \pm \vec{q}|/\mu$, $\rho = |\omega|/\mu$ and $\kappa = \frac{\pi}{4} \frac{m_D^2}{\mu^2}$. Transforming the integration variables from θ, \vec{r} to E_{\pm}, r_{\pm} , we end up with $I = \frac{1}{32\pi^4 \mu^2} \int_0 d\rho K(\rho)$ where

$$K(\rho) = \int dE_+ dE_- dr_+^2 dr_-^2 J \frac{r_+ r_- |E_+ E_- - \rho^2|}{(r_+^3 + \kappa|\rho|)(r_-^3 + \kappa|\rho|)(\rho^2 + E_+^2)(\rho^2 + E_-^2)}, \quad (4.58)$$

with the Jacobian

$$J = [(E_+ - E_-)^4 - 4(r_+^2 + r_-^2)(E_+ - E_-)^2 - 16(E_+ + E_-)^2 + 16r_+^2 r_-^2]^{-1/2}. \quad (4.59)$$

As $\rho \rightarrow 0$, we find that $K(\rho) \rightarrow \text{const} \times \rho^{-2/3}$ and $I = \text{finite}$. The absence of the forward singularity for the two gluon scattering vertex renders its contribution to the transition temperature smaller than the leading term by a factor of $g^2 / \ln \frac{\mu}{k_B T}$. Therefore its contribution is beyond the sub-sub-leading order according to the trade off (3.46).

V. LOFF PAIRING WITH A MISMATCHED FERMI SEA OF QUARKS.

A. A mismatched Fermi sea of quarks.

In the previous two sections, we took the massless limit of quarks, which is a good approximation at ultra-high baryon density. As the density is lowered, the nonzero masses of quarks have to be taken into account and different flavors will not have the same Fermi momentum. The phase space available for pairing will be reduced and new orders may arise. Crystalline color superconductivity discussed in [34] is a potential candidate.

In order to see how the Fermi sea of quarks is mismatched because of nonzero masses. consider the equilibrium of u, d, s quarks and electrons. The number density of each flavor is

$$n_f = \frac{k_f^3}{\pi^2} \quad (5.1)$$

where k_f the Fermi momentum of each flavor with $f = u, d, s$. The number density of electrons is $n_e = \frac{k_e^3}{3\pi^2}$ with k_e the Fermi momentum of electrons. The extra factor 3 for n_f comes from the three colors. Ignoring the interactions, the total energy at $T = 0$ is

$$E = \frac{3}{\pi^2} \int_0^{k_u} dp p^2 \sqrt{p^2 + m_u^2} + \frac{3}{\pi^2} \int_0^{k_d} dp p^2 \sqrt{p^2 + m_d^2} + \frac{3}{\pi^2} \int_0^{k_s} dp p^2 \sqrt{p^2 + m_s^2} + \frac{1}{\pi^2} \int_0^{k_e} dp p^2 \sqrt{p^2 + m_e^2}, \quad (5.2)$$

The total baryon number of the system is

$$b = \frac{1}{3}(n_u + n_d + n_s) \quad (5.3)$$

and the electric neutrality reads

$$\frac{2}{3}n_u - \frac{1}{3}n_d - \frac{1}{3}n_s - n_e = 0. \quad (5.4)$$

The Fermi momenta k_f and k_e are determined by minimizing the energy (5.2) subject to the constraints (5.3) and (5.4),

$$\frac{\partial F}{\partial k_f} = 0 \quad \frac{\partial F}{\partial k_e} = 0, \quad (5.5)$$

where

$$F = E - \frac{1}{3}\mu_B(n_u + n_d + n_s) - \mu_Q\left(\frac{2}{3}n_u - \frac{1}{3}n_d - \frac{1}{3}n_s - n_e\right) \quad (5.6)$$

with μ_B and μ_Q two Lagrangian multiplier. Under the approximation $k_f \gg m_f$, we end up with slightly different Fermi momenta for different flavors.

$$\begin{aligned} k_u &= k_F \\ k_d &= k_F + \frac{m_s^2 - m_d^2}{4k_F} \\ k_s &= k_F + \frac{m_d^2 - m_s^2}{4k_F}. \end{aligned} \quad (5.7)$$

where $k_F = \pi^{\frac{2}{3}}b^{\frac{1}{3}}$ is the universal Fermi momentum in the chiral limit. As the baryon density is lowered further such that $k_F \sim m_s$, more electrons will be involved for the electric neutrality.

B. Pairing instability at a nonzero total momentum.

A mismatched Fermi sea is known in a metallic superconductor with ferromagnetic impurities. The exchange interaction between the electron spins and the impurity spins displaces the Fermi momentum of each spin while levels up the total energy (kinetic and exchange) of each electron on the Fermi surface. The phase space available for BCS pairing (pairing between the electrons of momentum $\pm \vec{p}$) is reduced and other pairing states may arise. A potential candidate of them is that suggested by Larkins, Ovchinnikov, Fudde and Ferrell (LOFF) which pairs the electrons of momenta not exactly equal and opposite to each other

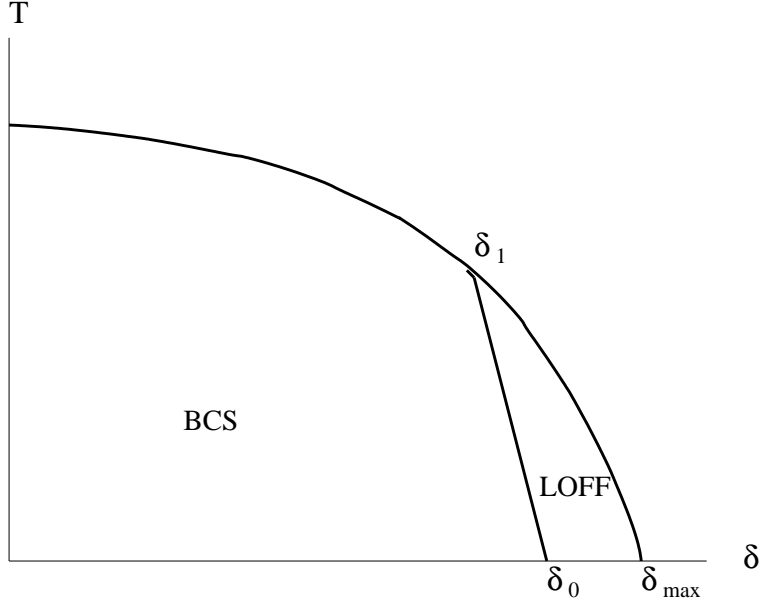


FIG. 9. The phase diagram showing the competition between BCS pairing and LOFF pairing.

[35]. The resultant Cooper pair in this case carries a net momentum, $2\vec{q}$, and the gap parameter supports a crystalline structure in the coordinate space,

$$\Delta(\vec{r}) = \Delta_0 e^{2i\vec{q}\cdot\vec{r}}. \quad (5.8)$$

Denoting the difference between the Fermi momenta of the two pairing quarks by 2δ , the phase diagram on the $T - \delta$ plane that shows the competition between BCS pairing and LOFF pairing is displayed in Fig. 9. At zero temperature, BCS state persists for $0 < \delta < \delta_0$ and LOFF state wins for $\delta_0 < \delta < \delta_{\max}$. Along the line of superconducting transition, it is from the normal phase to BCS phase for $0 < \delta < \delta_1$ and it is from the normal phase to LOFF phase for $\delta_1 < \delta < \delta_{\max}$. No long range orders exist for δ beyond δ_{\max} . The BCS phase and the LOFF phase below the transition temperature are separated by a first order phase transition.

The Dyson-Schwinger equation of section II can be easily generalized to the diquark scattering at a nonzero total momentum, i.e.

$$\Gamma_{\vec{q};\delta}(P_f|P_i) = \tilde{\Gamma}_{\vec{q},\delta}(P_f|P_i) + \frac{1}{\beta} \sum_{\nu} \int \frac{d^3 \vec{p}}{(2\pi)^3} K_{\vec{q};\delta}(P_f|P) \Gamma_{\vec{q};\delta}(P|P_i) \quad (5.9)$$

where the kernel is given by

$$K_{\vec{q};\delta}(P'|P) = \tilde{\Gamma}_{\vec{q},\delta}(P'|P) \mathcal{S}(Q + P, \mu + \delta) \mathcal{S}(Q - P, \mu - \delta) \quad (5.10)$$

with $\tilde{\Gamma}$ the 2PI part of the scattering vertex. The letter P 's in (5.9) stand for the relative four momenta between the pairing quarks with $P = (\vec{p}, -\nu)$ and the letter Q for their average four momentum with $Q = (\vec{q}, 0)$ (total momentum being $2Q$). The color-flavor and spinor indices have been suppressed, and the Fermi momentum of each quark propagator is indicated explicitly. The eigenvalue problem of the kernel reads

$$Ef(P) = \frac{1}{\beta} \sum_{\nu'} \int \frac{d^3 \vec{p}'}{(2\pi)^3} K_{\vec{q},\delta}(P|P') f(P'). \quad (5.11)$$

The maximum eigenvalue is a function of T , μ , δ and q and the pairing instability is given by the condition

$$E_{\max.}(T, \mu, \delta, q) = 1, \quad (5.12)$$

which gives the pairing temperature as a function of μ , δ and q , i.e. $T_{\text{pair}}(\mu, \delta, q)$. The transition temperature for a given μ and δ is determined by

$$T_c = \max(T_{\text{pair}}(\mu, \delta, q) | \forall q). \quad (5.13)$$

If this occurs at $q = 0$, the superconducting state below T_c is of BCS type. If this occurs at $q \neq 0$ the superconducting state below T_c is of LOFF type.

In the next subsection, we shall tackle the eigenvalue problem (5.11) for a point interaction and reproduce the results known to condensed matter physicist [36]. The solution for QCD will be presented in the last subsection, where we shall show how the forward singularity of the one-gluon exchange widens the LOFF window in the phase diagram on $T - \delta$ plane [37] [38] and distorts the shape of the order parameter below the transition [38].

C. LOFF pairing for a point interaction.

Consider the Hamiltonian with two species of fermions with different Fermi momenta interacting with each other via a point interaction, i.e.

$$H = \sum_{\vec{p}} [(p - \mu - \delta) a_{\vec{p}}^\dagger a_{\vec{p}} + (p - \mu + \delta) b_{\vec{p}}^\dagger b_{\vec{p}}] - \frac{1}{\Omega} \sum_{\vec{p}', \vec{p}, \vec{q}} G_{\vec{p}', \vec{p}} a_{\vec{q} + \vec{p}}^\dagger b_{\vec{q} - \vec{p}'}^\dagger b_{\vec{q} - \vec{p}} a_{\vec{q} + \vec{p}} \quad (5.14)$$

with $G_{\vec{p}', \vec{p}} = G\theta(\omega_0 - |p' - \mu|)\theta(\omega_0 - |p - \mu|)$ and $G > 0$. The 2PI vertex in this case is

$$\tilde{\Gamma}_{\vec{q},\delta}(P'|P) = -G\theta(\omega_0 - |p' - \mu|)\theta(\omega_0 - |p - \mu|) \quad (5.15)$$

and the kernel (5.10) reads

$$K_{\vec{q},\delta}(P'|P) = -G\theta(\omega_0 - |p' - \mu|)\theta(\omega_0 - |p - \mu|)S(Q + P, \mu + \delta)S(Q - P, \mu - \delta) \quad (5.16)$$

with

$$S(P, \mu) = \frac{i}{i\nu - p + \mu}. \quad (5.17)$$

Only the zero angular momentum channel is present for pairing.

The integral equation (5.11) is completely separable and admits an exact solution. There is only one nonzero eigenvalue given by

$$E = 1 + \frac{1}{\ln \frac{2\omega_0}{\Delta_0}} \left[\ln \frac{\Delta_0}{\pi k_B T} + \gamma + \psi\left(\frac{1}{2}\right) - \frac{\pi k_B T}{q} \operatorname{Im} \ln \frac{\Gamma\left(\frac{1}{2} - \frac{i(\delta-q)}{2\pi k_B T}\right)}{\Gamma\left(\frac{1}{2} - \frac{i(\delta+q)}{2\pi k_B T}\right)} \right], \quad (5.18)$$

where Δ_0 is the energy gap at $T = 0$, $\delta = 0$ and $q = 0$. The corresponding eigenfunction is

$$f(P) = \left[\frac{1}{4\pi^2} \left(\ln \frac{2\omega_0}{k_B T} + \gamma \right) \right]^{-\frac{1}{2}} \theta(\omega_0 - |p - \mu|). \quad (5.19)$$

The eigenvalue problem (5.11) can also be solved by the perturbation theory developed in section III with the kernel of the zeroth order given by (5.16) at $\delta = 0$ and $\vec{q} = 0$ and the perturbation by

$$\begin{aligned} \Delta K(P'|P) &= K_{\delta, \vec{q}}(P'|P) - K_{0,0}(P'|P) \\ &= -G\theta(\omega_0 - |p' - \mu|)\theta(\omega_0 - |p - \mu|)[S(Q + P, \mu + \delta)S(Q - P, \mu - \delta) - S(P, \mu)S(-P, \mu)]. \end{aligned} \quad (5.20)$$

Eq.(5.19) is the eigenfunction of both the zeroth order kernel and the perturbation. Thus the first order perturbation gives rise to the exact eigenvalue (5.18).

The pairing instability is located according to the equation $E_{\max} = 1$, i.e.

$$\left[\ln \frac{\Delta_0}{\pi k_B T} + \gamma + \psi\left(\frac{1}{2}\right) - \frac{\pi k_B T}{q} \operatorname{Im} \ln \frac{\Gamma\left(\frac{1}{2} - \frac{i(\delta-q)}{2\pi k_B T}\right)}{\Gamma\left(\frac{1}{2} - \frac{i(\delta+q)}{2\pi k_B T}\right)} \right] = 0, \quad (5.21)$$

with $\psi(z) = \frac{d \ln \Gamma(z)}{dz}$ and the transition temperature is determined by (5.13) [36]. The numerical solution to (5.21) yields the values of relevant parameters in the phase diagram Fig. 9.

$$\begin{aligned} \delta_1 &= 0.606\Delta_0 \\ \delta_{\max} &= 0.745\Delta_0. \end{aligned} \quad (5.22)$$

The BCS state amounts to pair quarks of equal and opposite momenta at disadvantage of the mismatched Fermi sea. The quasi particle operator is related to $a_{\vec{p}}$ and $b_{\vec{p}}$ by a Bogoliubov transformation

$$\begin{pmatrix} \alpha_{\vec{p}} \\ \beta_{-\vec{p}}^\dagger \end{pmatrix} = \begin{pmatrix} u_{\vec{p}} & -v_{\vec{p}} \\ v_{\vec{p}} & u_{\vec{p}} \end{pmatrix} \begin{pmatrix} a_{\vec{p}} \\ b_{-\vec{p}}^\dagger \end{pmatrix}. \quad (5.23)$$

with

$$\begin{aligned} u_{\vec{p}}^2 &= \frac{1}{2} \left[1 + \frac{p - \mu}{\sqrt{(p - \mu)^2 + \Delta^2}} \right] \\ v_{\vec{p}}^2 &= \frac{1}{2} \left[1 - \frac{p - \mu}{\sqrt{(p - \mu)^2 + \Delta^2}} \right] \end{aligned} \quad (5.24)$$

The ground state, $|\text{BCS}\rangle$, is annihilated by α or β of an arbitrary momentum. The quasi particle energy

$$E_{\vec{p}}^{\pm} = \pm\delta + \sqrt{(p - \mu)^2 + \Delta^2} \quad (5.25)$$

opens a gap $\Delta - \delta$ for $\delta < \Delta$.

The LOFF state amounts to pair the quark of momentum $\vec{q} + \vec{p}$ with that of $\vec{q} - \vec{p}$ and the quasi particle operator is given by a modified Bogoliubov transformation:

$$\begin{pmatrix} \alpha_{\vec{q}+\vec{p}} \\ \beta_{\vec{q}-\vec{p}}^\dagger \end{pmatrix} = \begin{pmatrix} u_{\vec{p}} & -v_{\vec{p}} \\ v_{\vec{p}} & u_{\vec{p}} \end{pmatrix} \begin{pmatrix} a_{\vec{q}+\vec{p}} \\ b_{\vec{q}-\vec{p}}^\dagger \end{pmatrix}. \quad (5.26)$$

The quasi particle energy is

$$E_{\vec{p}}^{\pm} = \pm(q \cos \theta + \delta) + \sqrt{(p - \mu)^2 + \Delta^2} \quad (5.27)$$

with θ the angle between \vec{p} and \vec{q} and can be negative. The corresponding ground state reads

$$|\text{LOFF}\rangle = \prod_{E_{\vec{p}}^+ < 0} \alpha_{\vec{p}}^\dagger \prod_{E_{\vec{p}}^- < 0} \beta_{\vec{p}}^\dagger | \rangle \quad (5.28)$$

with the state $| \rangle$ annihilated by α and β for all \vec{p} . Upon comparison between the free energy of a BCS state and that of a LOFF state at $T = 0$, we find that BCS state extends to $\delta \simeq \frac{\Delta_0}{\sqrt{2}}$ and is replaced by LOFF states up to δ_{max} . The BCS state and the LOFF state are separated by a first-order phase transition. Using Ginzburg-Landau approximation to the gap equation, the authors of [39] argued that the transition from the normal phase to LOFF phase is also of the first order because of the negative quartic term for certain crystalline structures of the LOFF state.

D. LOFF pairing with one gluon exchange.

Consider an idealized problem of two flavor pairing, $N_f = 2$, with a Fermi-momentum difference 2δ . The vertex function of one-gluon exchange within the color anti-symmetric channel and with a total spatial momentum $2\vec{q}$, $\Gamma_{\vec{q},\delta}(P'|P)$, contains all angular momentum channels and reduces to Γ^A of (3.7) at $\vec{q} = 0$ and $\delta = 0$. The corresponding kernel of Dyson-Schwinger equation for di-quark scattering, eq. (5.10), is diagonalized perturbatively in sections III and IV under the same condition. The maximum eigenvalue within each angular momentum channel given by

$$E_{\text{max.}}^J = 1 + \frac{2}{\ln \frac{1}{\epsilon}} \left(\ln \frac{\Delta_0}{\pi k_B T} + \gamma + 6s_J \right) + O\left(\ln^{-2} \frac{1}{\epsilon}\right), \quad (5.29)$$

where

$$\epsilon = \frac{g^5 k_B T_c}{256 \pi^3 \mu}, \quad (5.30)$$

with T_c referring to the transition temperature at $\delta = 0$, Δ_0 is the energy gap at $T = 0$ and $\delta = 0$, and $E_{\text{max.}}^J$ here is the same as E_0 of eq.(4.21) for $N_f = 2$. The corresponding eigenfunction to the leading order reads

$$f_{JM}(P) = C \sin\left(\frac{\pi \ln \frac{1}{\nu}}{2 \ln \frac{\Delta_0 e^\gamma}{\pi \epsilon k_B T}}\right) \frac{Y_{JM}(\theta, \phi)}{p} \quad (5.31)$$

with $Y_{JM}(\theta, \phi)$ the ordinary spherical harmonics. The adjoint of (5.31) is given by

$$\bar{f}_{JM}(P) = \frac{f_{JM}^*(P)}{\nu^2 + (p - \mu)^2} \quad (5.32)$$

and the constant C of (5.31) is determined by the normalization condition

$$\frac{1}{\beta} \sum_\nu \int \frac{d^3 \vec{p}}{(2\pi)^3} \bar{f}(P) f(P) = 1. \quad (5.33)$$

Near the transition, $\ln \frac{1}{\epsilon} = O(g^{-1})$. We notice that the dependence on the angular momentum is of the sub-leading order. In another word, maximum eigenvalues of different angular momenta are all degenerate to the leading order as a consequence of the forward singularity.

We shall treat the case with $\vec{q} \neq 0$ and $\delta \neq 0$ with the aid of the perturbation method developed in sections III and IV. The perturbing kernel is

$$\begin{aligned} \Delta K(P'|P) &= K_{\vec{q}, \delta}(P'|P) - K_{0,0}(P'|P) \\ &= [\tilde{\Gamma}_{\vec{q}, \delta}(P'|P) - \tilde{\Gamma}_{0,0}(P'|P)] S(P, \mu) S(-P, \mu) \\ &= \tilde{\Gamma}_{0,0}(P'|P) [S(Q + P, \mu + \delta) S(Q - P, \mu - \delta) - S(P, \mu) S(-P, \mu)] \\ &= [\tilde{\Gamma}_{\vec{q}, \delta}(P'|P) - \tilde{\Gamma}_{0,0}(P'|P)] [S(Q + P, \mu + \delta) S(Q - P, \mu - \delta) - S(P, \mu) S(-P, \mu)]. \end{aligned} \quad (5.34)$$

Since the relevant momentum scale of the vertex function is μ , the difference $[\tilde{\Gamma}_{\vec{q}, \delta}(P'|P) - \tilde{\Gamma}_{0,0}(P'|P)]$ is expected to be higher than $\tilde{\Gamma}_{0,0}(P'|P)$ by the order of $O\left(\frac{\Delta_0^2}{\mu^2}\right)$. The only contribution to the sub-leading term comes from the propagator difference $[S(Q + P, \mu + \delta) S(Q - P, \mu) - S(P, \mu - \delta) S(-P, \mu)]$, similar to the case of a point interaction. If $\vec{q} = 0$, rotation symmetry is maintained. The shift of the eigenvalue is simply the expectation value of the perturbing kernel, like the case of the point interaction and we end up with

$$\delta E = \frac{2}{\ln \frac{1}{\epsilon}} \left[\psi\left(\frac{1}{2}\right) - \psi\left(\frac{1}{2} - i \frac{\delta}{2\pi k_B T}\right) \right], \quad (5.35)$$

where the second term inside the bracket corresponds to the limit $q \rightarrow 0$ of the logarithm of the ratio of gamma functions in (5.18). If $\vec{q} \neq 0$, the dependence of the perturbing kernel on the angle between the relative momentum and the total momentum breaks the rotational symmetry. Different angular momentum channels will be mixed and a degenerate perturbation theory has to be employed to figure out δE .

In general, the maximum eigenvalue of the kernel (5.16) can be written as

$$E_{\max} = 1 + \frac{2}{\ln \frac{1}{\epsilon}} \left(\ln \frac{\Delta_0}{\pi k_B T} + \gamma + \rho_{\max.} \right) + \text{sub-sub-leading terms} \quad (5.36)$$

with $\rho_{\max.}$ the maximum eigenvalue of the operator

$$h_{\text{op.}} = s_{\text{op.}} + v_{\text{op.}}. \quad (5.37)$$

	One-gluon exchange	Point interaction
Upper limit of LOFF window	$\delta_{\max} = 0.968\Delta_0$	$\delta_{\max} = 0.754\Delta_0$
Onset of LOFF along T_c	$\delta_1 = 0.606\Delta_0$	$\delta_1 = 0.606\Delta_0$
Onset of LOFF along $T = 0$	$\delta_0 < 0.707\Delta_0$	$\delta'_0 = 0.707\Delta_0$
Shape of the gap	non-spherical	spherical

TABLE II. The parameters underlying a LOFF pairing.

The operator $s_{\text{op.}}$ is diagonal in the angular momentum representation,

$$\langle J', M' | s_{\text{op.}} | JM \rangle = 6s_J \delta_{J'J} \delta_{M'M}, \quad (5.38)$$

while the operator $v_{\text{op.}}$ is diagonal in the coordinate representation (angle representation),

$$\begin{aligned} v_{\text{op.}} &= \frac{1}{\beta^2} \sum_{\nu', \nu} \int \frac{d^3 \vec{p}'}{(2\pi)^3} \int \frac{d^3 \vec{p}}{(2\pi)^3} \bar{f}(\nu', p') \Delta K(P'|P) f(\nu, p) \\ &= \psi\left(\frac{1}{2}\right) - \text{Re}\psi\left[\frac{1}{2} - i\frac{\delta - q \cos \theta}{2\pi k_B T}\right] \end{aligned} \quad (5.39)$$

In the coordinate representation, the eigenvalue equation $h_{\text{op.}} u = \rho u$ takes the form [38]

$$3 \int_{-1}^1 dx' \frac{u(x) - u(x')}{|x - x'|} = \left\{ \psi\left(\frac{1}{2}\right) - \text{Re}\psi\left[\frac{1}{2} - i\frac{\delta - qx}{2\pi k_B T}\right] \right\} u(x) = \rho u(x) \quad (5.40)$$

with $x = \cos \theta$. For $q \neq 0$, this integral equation can only be solved numerically and we obtain the values of the parameters in the phase diagram Fig. 9, i.e.

$$\begin{aligned} \delta_1 &= 0.606\Delta_0 \\ \delta_{\max.} &= 0.968\Delta_0. \end{aligned} \quad (5.41)$$

Our result for $\delta_{\max.}$ is different from that of Ref. [37], which claims that $\delta_{\max.} = \infty$. The eigenfunction $u(\cos \theta)$ corresponding to $\delta_{\max.}$ is plotted in Fig. 10. This is to replace the spherical harmonics in (5.31) for $M = 0$ for the zeroth order eigenfunction of the degenerate perturbation theory.

The widening of the LOFF window comes from the angular momentum mixing, which is another consequence of the forward singularity. Furthermore the gap parameter right below the transition line follows the shape of the eigenfunction $u(x)$ and is no longer spherical for $\delta > \delta_1$ as is shown in Fig. 10. Because of the flexibility of the shape of the gap parameter for LOFF pairing via the angular momentum mixing, the other end of the LOFF window at $T = 0$ is expected to be lower than that for a point interaction, i.e. $\delta_0 < \frac{\Delta_0}{\sqrt{2}}$.

The parameters underlying the LOFF pairing for one-gluon exchange and that for a point interaction are summarized in Table II for comparison.

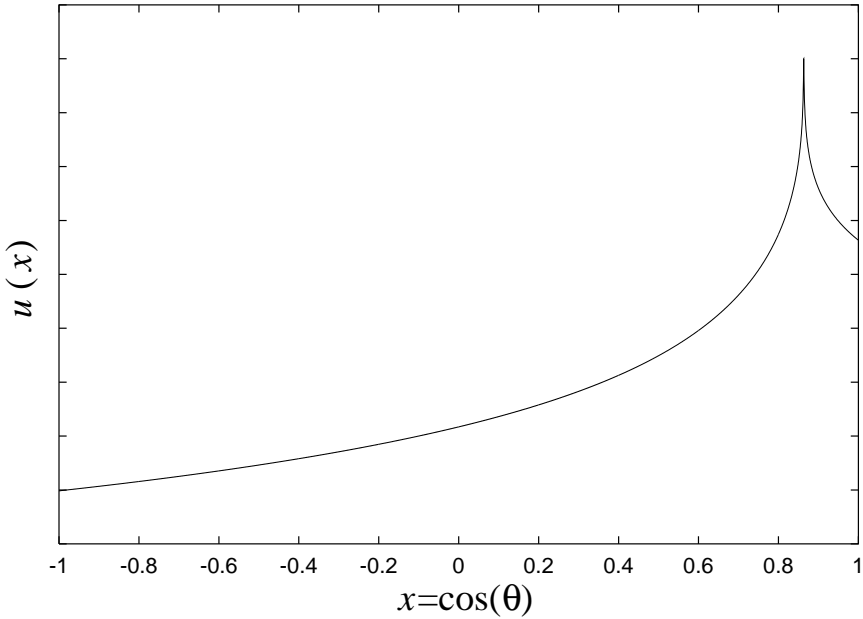


FIG. 10. The eigenfunction $u(x)$ corresponding to the largest eigenvalue of Eq. (5.40).

VI. GINZBURG LANDAU THEORY OF COLOR SUPERCONDUCTIVITY.

A. The general structure.

Like a metallic superconductor, the physics of a color superconductor near the critical temperature can be described in terms of Ginzburg-Landau free energy [40]. Ginzburg-Landau theory is also a powerful tool to explore an inhomogeneous condensate as induced by an external field or by a nontrivial boundary condition, e. g. a vortex filament or a domain wall. Though derivable from the first-principle QCD Lagrangian in the weak coupling limit, the validity of the Ginzburg-Landau theory is not restricted within the perturbative region if the coefficients involved are regarded phenomenological

The symmetry of QCD with three flavors u , d and s in the chiral limit is $SU(3)_c \times SU(3)_R \times SU(3)_L \times U(1)_B$ with the ordinary electromagnetic $U(1)$ a subgroup of the flavor $SU(3)$ i.e. $U(1)_{\text{em}} \subset SU(3)_R \times SU(3)_L$. As was analyzed in previous sections, the most favorable pairing configuration is between two quarks of equal helicity at zero angular momentum. The corresponding order parameter $\Psi_R(\Psi_L)$ for right (left) handed Cooper pairs carries the color-flavor indices of each pairing quark, i.e $(\Psi_{R(L)})_{f_1 f_2}^{c_1 c_2}$ and is symmetric under a simultaneous interchange of them, i. e.

$$(\Psi_{R(L)})_{f_1 f_2}^{c_1 c_2} = (\Psi_{R(L)})_{f_2 f_1}^{c_2 c_1}. \quad (6.1)$$

Since the pairing channel is $\bar{\mathbf{3}}$, the order parameter is expected to be approximately anti-symmetric with respect to interchanging the two color indices, i.e.

$$(\Psi_{R(L)})_{f_1 f_2}^{c_1 c_2} \simeq -(\Psi_{R(L)})_{f_1 f_2}^{c_2 c_1}. \quad (6.2)$$

It follows from (6.1) that

$$(\Psi_{R(L)})_{f_1 f_2}^{c_1 c_2} \simeq -(\Psi_{R(L)})_{f_2 f_1}^{c_1 c_2}. \quad (6.3)$$

A small color-symmetric (sextet) component of the order parameter can be induced but its contribution to the free energy is of higher order as is analyzed in the appendix C. Dropping the color symmetric component, the most general form of the Ginzburg-Landau free energy functional consistent with the symmetry is

$$\begin{aligned} \Gamma = \int d^3 \vec{r} \{ & \frac{1}{4} F_{ij}^l F_{ij}^l + \frac{1}{2} (\vec{\nabla} \times \vec{A})^2 + \frac{1}{2} \text{Tr}[(\vec{D}\Psi_R)^\dagger (\vec{D}\Psi_R) + (\vec{D}\Psi_L)^\dagger (\vec{D}\Psi_L)] \\ & + \frac{1}{2} a \text{Tr}[\Psi_R^\dagger \Psi_R + \Psi_L^\dagger \Psi_L] + \frac{1}{4} b \text{Tr}[(\Psi_R^\dagger \Psi_R)^2 + (\Psi_L^\dagger \Psi_L)^2] \\ & + \frac{1}{4} b' [(\text{Tr}\Psi_R^\dagger \Psi_R)^2 + (\text{Tr}\Psi_L^\dagger \Psi_L)^2] + c \text{Tr}(\Psi_R^\dagger \Psi_R) \text{Tr}(\Psi_L^\dagger \Psi_L) \} \end{aligned} \quad (6.4)$$

where the gauge covariant derivative of the diquark condensate Ψ reads

$$\begin{aligned} (\vec{D}\Psi_{R(L)})_{f_1 f_2}^{c_1 c_2} = & \vec{\nabla}(\Psi_{R(L)})_{f_1 f_2}^{c_1 c_2} - ig \vec{A}^{c_1 c'} (\Psi_{R(L)})_{f_1 f_2}^{c' c_2} - ig \vec{A}^{c_2 c'} (\Psi_{R(L)})_{f_1 f_2}^{c_1 c'} \\ & - ie(q_{f_1} + q_{f_2}) \vec{\mathcal{A}}(\Psi_{R(L)})_{f_1 f_2}^{c_1 c_2} \end{aligned} \quad (6.5)$$

with $\vec{A} = \vec{A}^l T^l$ the color gauge potential, $\vec{\mathcal{A}}$ the electromagnetic one and the trace is defined by $\text{Tr}MN \equiv M_{f_1 f_2}^{c_1 c_2} N_{f_2 f_1}^{c_2 c_1}$. Parity violating terms are neglected in (6.4) and an even parity condensate,

$$\Psi_R = \Psi_L \equiv \Psi$$

will be considered in subsequent discussions. The variational minimum of (6.4) with respect to the gauge potentials and the di-quark condensates satisfies a set nonlinear Ginzburg-Landau equations whose solution gives rise to the equilibrium configuration of the mean field Ψ , \vec{A} and $\vec{\mathcal{A}}$.

On writing

$$\Psi_{f_1 f_2}^{c_1 c_2} = \epsilon^{c_1 c_2 c} \epsilon_{f_1 f_2 f} \Phi_f^c \quad (6.6)$$

with Φ a 3×3 complex matrix supporting the representation $\mathbf{1} \oplus \mathbf{8}$ under a simultaneous color-flavor rotation, the Ginzburg-Landau free energy becomes

$$\Gamma = \int d^3 \vec{r} \left[\frac{1}{4} F_{ij}^l F_{ij}^l + \frac{1}{2} (\vec{\nabla} \times \vec{A})^2 + 4 \text{tr}(\vec{D}\Phi)^\dagger (\vec{D}\Phi) + 4a \text{tr}\Phi^\dagger \Phi + b_1 \text{tr}(\Phi^\dagger \Phi)^2 + b_2 (\text{tr}(\Phi^\dagger \Phi))^2 \right], \quad (6.7)$$

where $b_1 = b$, $b_2 = b + 8b' + 8c$,

$$\vec{D}\Phi = \vec{\nabla}\Phi - ig \vec{A}^l \bar{T}^l \Phi - iq \mathcal{A} \Phi Q \quad (6.8)$$

with \bar{T}^l the generator in $\bar{\mathbf{3}}$ and the charge matrix

$$Q = \text{diag}\left(\frac{2}{3}, -\frac{1}{3}, -\frac{1}{3}\right) = -\frac{2}{\sqrt{3}} \bar{T}^8. \quad (6.9)$$

The trace, $\text{tr}(\dots)$, refers now to 3×3 matrices and we have rearranged the $SU(3)$ generator to make \bar{T}_8 proportional to the charge matrix.

In the weak coupling limit, the Ginzberg-Landau coefficients can be derived from QCD one-gluon exchange or NJL effective Lagrangian and we have [41] [25]

$$\begin{aligned} a &= \frac{48\pi^2}{7\zeta(3)} k_B^2 T_c (T - T_c) \\ b &= \frac{576\pi^4}{7\zeta(3)} \left(\frac{k_B T_c}{\mu} \right)^2 \\ b' &= c = 0. \end{aligned} \quad (6.10)$$

For a homogeneous color superconductor, eq. (6.7) becomes

$$\Gamma = \Omega [4a\text{tr}\Phi^\dagger\Phi + b_1\text{tr}(\Phi^\dagger\Phi)^2 + b_2(\text{tr}(\Phi^\dagger\Phi))^2]. \quad (6.11)$$

Depending on the coefficients of the quartic term, there are three different cases of the variational minimum of (6.11) [41] [25]:

1) $b_1 > 0$ and $b_1 + 3b_2 > 0$: The minimization of (6.11) produces

$$\Phi = \phi_{\text{CFL}} U \quad (6.12)$$

with

$$\phi_{\text{CFL}} = \sqrt{-\frac{2a}{b_1 + 3b_2}} \quad (6.13)$$

and U an arbitrary unitary matrix. The order parameter supports the unit representation of the simultaneous color-flavor rotation and is therefore color-flavor locked. For $U = 1$, we obtain the standard form of the order parameter (2.22), with $\phi_S = 0$ and $\phi_A = \phi_{\text{CFL}}$. The minimum free energy density reads

$$\frac{\Gamma_{\text{min.}}}{\Omega} = -\frac{12a^2}{b_1 + 3b_2} = -\frac{12\mu^2}{7\zeta(3)} (k_B T_c)^2 \left(\frac{T_c - T}{T_c} \right)^2, \quad (6.14)$$

where the last equality follows from the substitution of the weak coupling coefficients (6.10). We shall consider this region of parameters only for the rest of the section.

Although a homogeneous CFL condensate can always be transformed to the standard form with $U = 1$ by a symmetry operation of (2.19), it is no longer the case in the presence of a vortex filament, which implement a nontrivial mapping of $\pi_1(U)$ [25].

2) $b_1 < 0$ and $b_1 + b_2 > 0$

The variational solution in this case reads

$$\Phi = \text{diag}(0, 0, \phi_{\text{IS}} e^{i\alpha}) \quad (6.15)$$

with

$$\phi_{\text{IS}} = \sqrt{-\frac{2a}{b_1 + b_2}} \quad (6.16)$$

and the minimum free energy is

$$\frac{\Gamma_{\min.}}{\Omega} = -\frac{4a^2}{b_1 + b_2}. \quad (6.17)$$

This case corresponds to an isoscalar [41]. Notice that the trace of (6.15) may be transformed away upon a flavor $SU(3)$ rotation, e.g. $\Phi \rightarrow \Phi U$ with

$$U = \begin{pmatrix} 1 & 0 & 0 \\ 0 & 0 & -1 \\ 0 & 1 & 0 \end{pmatrix}. \quad (6.18)$$

Therefore this condensate belongs to the octet under a simultaneous color-flavor rotation.

3) Other regions of the quartic coefficients:

The stationary point of Γ becomes a saddle points and higher order terms of Ginzburg-Landau free energy have to be restored to stabilize the condensate.

B. Characteristic lengths of a color superconductor.

To identify various length scale that characterize an inhomogeneous condensate, we consider small fluctuations about the homogeneous one (6.11). We parametrize the order parameter by

$$\Phi = \phi_{\text{CFL}} + \frac{1}{\sqrt{6}}\left(\frac{X + iY}{2}\right) + \bar{T}^l\left(\frac{X_l + iY_l}{2}\right) \quad (6.19)$$

with X 's and Y 's real, and form linear combinations of the ordinary electromagnetic gauge potential with the eighth component of the colour gauge potential

$$\begin{aligned} \vec{V} &= \vec{A}_8 \cos \theta + \vec{\mathcal{A}} \sin \theta \\ \vec{\mathcal{V}} &= -\vec{A}_8 \sin \theta + \vec{\mathcal{A}} \cos \theta, \end{aligned} \quad (6.20)$$

where the 'Weinberg angle' is given by

$$\tan \theta = -\frac{2e}{\sqrt{3}g}, \quad (6.21)$$

Next, the free energy (6.7) is expanded to quadratic order in X 's Y 's \vec{A} 's and \mathcal{A} . We find that

$$\begin{aligned} \Gamma &= \Gamma_{\min} + \int d^3\vec{r} \left\{ \frac{1}{2}(\vec{\nabla} \times \vec{V})^2 + \text{tr}[(\vec{\nabla} \times \vec{W})^2 + m_W^2 \vec{W}^2] + \frac{1}{2}[(\vec{\nabla} \times \vec{Z})^2 + m_Z^2 \vec{Z}^2] \right. \\ &\quad \left. + \frac{1}{2}[(\vec{\nabla} X)^2 + m_H^2 X^2] + \frac{1}{2}[(\vec{\nabla} X^l)(\vec{\nabla} X^l) + m_H'^2 X^l X^l] + \frac{1}{2}(\vec{\nabla} Y)^2 \right\}, \end{aligned} \quad (6.22)$$

where $\vec{W} = \sum_{l=1}^7 \bar{T}^l \vec{W}^l$ and

$$\begin{aligned}\vec{W}^l &= \vec{A}^l - \frac{1}{m_W} \vec{\nabla} Y^l \quad \text{for } l = 1, 2, \dots, 7 \\ \vec{Z} &= \vec{V} - \frac{1}{m_Z} \vec{\nabla} Y^8,\end{aligned}\tag{6.23}$$

The masses of the excitations provide us with the relevant length scales which are the coherence lengths, ξ and ξ' defined by:

$$m_H^2 = (b_1 + 3b_2)\phi_{\text{CFL}}^2 = \frac{2}{\xi^2}, \quad m_H'^2 = b_1\phi_{\text{CFL}}^2 = \frac{2}{\xi'^2},\tag{6.24}$$

that indicate the distances over which the diquark condensate varies and the magnetic penetration depths, δ and δ' by

$$m_Z^2 = 4g^2\phi_{\text{CFL}}^2 \sec^2 \theta = \frac{1}{\lambda^2}, \quad m_W^2 = m_Z^2 \cos^2 \theta = \frac{1}{\lambda'^2}.\tag{6.25}$$

The Ginzburg-Landau parameter that classifies the types of the response of the superconductor to an external magnetic field is defined by the ratio

$$\kappa = \frac{\lambda}{\xi}\tag{6.26}$$

and we shall see in the next subsection that the critical value that separates the type I superconductivity and the type II one is different from that of an metallic superconductor because of the multiplicity of the order parameter.

The fluctuations considered so far are all of even parity, i.e. the relation $\Psi_R = \Psi_L$ is maintained. The excitations that violate this relation are of odd parity and correspond to the Goldstone bosons associated with the chiral symmetry breaking induced by CFL.

C. The magnetic response and the types of the color superconductivity.

Before discussing the inhomogeneous condensation of a domain wall, we shall first determine the thermodynamical critical magnetic field of a homogeneous condensation with color-flavor locking.

Like an metallic superconductor, the thermal equilibrium in a constant external magnetic field \vec{H} is determined by Gibbs free energy, which is a Legendre transformation of (6.7), i.e.

$$\tilde{\Gamma} = \Gamma - \vec{H} \cdot \int d^3r \vec{\nabla} \times \vec{\mathcal{A}} = \tilde{\Gamma}_1 + \tilde{\Gamma}_2,\tag{6.27}$$

where

$$\begin{aligned}\tilde{\Gamma}_1 &= \int d^3r \left[\frac{1}{4} \sum_{l=1}^7 F_{ij}^l F_{ij}^l + \frac{1}{2} (\vec{\nabla} \times \vec{V})^2 + 4\text{tr}(\vec{D}\Phi)^\dagger (\vec{D}\Phi) + 4a\text{tr}\Phi^\dagger \Phi \right. \\ &\quad \left. + b_1\text{tr}(\Phi^\dagger \Phi)^2 + b_2(\text{tr}(\Phi^\dagger \Phi))^2 - \vec{H} \cdot \vec{\nabla} \times \vec{V} \sin \theta \right]\end{aligned}\tag{6.28}$$

and

	Super phase	Normal phase
Φ	ϕ_{CFL}	0
$\vec{\nabla} \times V$	0	$\vec{H} \sin \theta$
$F_{ij}^{1,\dots,7}$	0	0
Γ_1	$-\Omega \frac{12a^2}{b_1+3b_2}$	$-\Omega \frac{1}{2} H^2 \sin^2 \theta$

TABLE III. The comparison between the super phase and the normal phase in an external magnetic field.

$$\tilde{\Gamma}_2 = \int d^3 \vec{r} \left[\frac{1}{2} (\vec{\nabla} \times \vec{\mathcal{V}})^2 - \vec{H} \cdot \vec{\nabla} \times \vec{\mathcal{V}} \cos \theta \right]. \quad (6.29)$$

The minimization of $\tilde{\Gamma}_2$ with respect \mathcal{V} yields $\vec{\nabla} \times \vec{\mathcal{V}} = \vec{H} \cos \theta$ and $\tilde{\Gamma}_2 = -\frac{1}{2} \Omega H^2 \cos^2 \theta$. Since $\vec{\mathcal{V}}$ corresponds to the unbroken $U(1)$ gauge symmetry and does not couple to the order parameter, we shall concentrate our attention to $\tilde{\Gamma}_1$ from now on. The results of minimization of $\tilde{\Gamma}_1$ in the super phase and in the normal phase are summarized in Table III.

The thermodynamical critical field is determined by the condition $(\tilde{\Gamma}_1)_n = (\tilde{\Gamma}_1)_s$ and we obtain that [42]

$$H_c = 2 \sqrt{\frac{6a^2}{b_1 + 3b_2}} \csc \theta \quad (6.30)$$

A first order phase transition from the super phase to the normal phase occurs for a type I superconductor when the external field exceeds this magnitude.

To determine the type of a color superconductor, we repeat the analysis in [40] for a metallic superconductor by considering a domain wall, i.e. a planar interface between the super phase with CFL and the normal phase. The bulk equilibrium is maintained by an external magnetic field tuned at the critical magnitude (6.30). The surface tension of the domain wall is defined by

$$\sigma \equiv \frac{\tilde{\Gamma}_1 - (\tilde{\Gamma}_1)_s}{\text{the area of the interface}} = \frac{\tilde{\Gamma}_1 - (\tilde{\Gamma}_1)_n}{\text{the area of the interface}}. \quad (6.31)$$

A positive σ favors homogeneity and the superconductor is of type I. A negative σ favors inhomogeneity and the superconductor is of type II. The critical value of the Ginzburg-Landau parameter is determined by the condition $\sigma = 0$ [43].

On writing $\Phi = \Phi_0 + \Phi_l \bar{T}^l$, we observe that there are no terms in $\tilde{\Gamma}_1$ that are linear in Φ_1, \dots, Φ_7 or $\vec{A}_1, \dots, \vec{A}_7$. A consistent solution to the Ginzburg-Landau equation that implements the maximum symmetry maintained by the external conditions amounts to set $\Phi_1 = \dots = \Phi_7 = 0$ and $\vec{A}_1 = \dots, \vec{A}_7 = 0$. Taking the coordinate system with the external magnetic field in z -direction and the interface parallel to yz -plane, the solution ansatz is taken to be

$$\begin{aligned} \Phi &= \frac{1}{3} \phi_{\text{CFL}} (u + 2v) + \frac{2}{\sqrt{3}} \phi_{\text{CFL}} (u - v) \bar{T}^8 \\ \vec{V} &= -\frac{\sqrt{-3a}}{g} A \hat{y} \cos \theta \end{aligned} \quad (6.32)$$

with u , v and A functions of x only. The boundary condition reads

$$(u, v) \rightarrow \begin{cases} 1 & \text{for } x \rightarrow \infty \\ 0 & \text{for } x \rightarrow -\infty \end{cases}, \quad (6.33)$$

and

$$\frac{dA}{dx} \rightarrow \begin{cases} 0 & \text{for } x \rightarrow \infty \\ -1 & \text{for } x \rightarrow -\infty \end{cases}. \quad (6.34)$$

In terms of the dimensionless field variables u , v and A , and the dimensionless coordinate $s = \frac{x}{\lambda}$, the surface tension becomes

$$\begin{aligned} \sigma = \frac{6a^2}{b} \lambda \int_{\infty}^{\infty} ds \left[\frac{1}{2}(A' - 1)^2 + \frac{1}{3\kappa^2}(u'^2 + 2v'^2) + \frac{1}{6}A^2(2u^2 + v^2) - \frac{1}{3}(u^2 + 2v^2) \right. \\ \left. + \frac{1}{18}(2u^4 + 2u^2v^2 + 5v^4) + \frac{1}{18}\rho(u^2 - v^2)^2 \right] \end{aligned} \quad (6.35)$$

with $f' = \frac{df}{ds}$, where κ is the Ginzburg-Landau parameter defined in (6.26) and

$$\rho = \frac{b_1 - 3b_2}{b_1 + 3b_2} \quad (6.36)$$

is another dimensionless parameter and is equal to $-\frac{1}{2}$ for perturbative coefficients (6.10). The minimization of (6.35) generates three coupled equations of motion, whose solution, when substituted back to (6.35) gives rise to the minimum surface tension, $\sigma_{\min.}(\kappa, \rho)$. The critical GL parameter that separate type I from type II is defined by the condition that

$$\sigma_{\min.}(\kappa, \rho) = 0. \quad (6.37)$$

The partial derivatives of $\sigma_{\min.}$ with respect to κ or ρ come only from the explicit dependence of (6.35) on them. The contribution from the implicit dependence on κ or ρ through u , v and A drops out because of the equations of motion. Therefore we have

$$\left(\frac{\partial \sigma_{\min.}}{\partial \kappa} \right)_{\rho} \leq 0 \quad (6.38)$$

and

$$\left(\frac{\partial \sigma_{\min.}}{\partial \rho} \right)_{\kappa} \geq 0. \quad (6.39)$$

Consider a special field configuration $u = v$, which satisfies the boundary conditions. This trial field configuration makes the surface tension (6.35) coincide with that of an metallic superconductor, for which the critical GL parameter is $\kappa = \frac{1}{\sqrt{2}} \simeq 0.707$ [40]. But the equations of motion may not be satisfied with $u = v$ everywhere and therefore $\sigma_{\min.} \leq 0$ at this κ . It follows then from (6.38) that the critical GL parameter for a color superconductor

$$\kappa_c(\rho) \leq \frac{1}{\sqrt{2}}. \quad (6.40)$$

Furthermore we have

$$\frac{d\kappa_c}{d\rho} = \left(\frac{\partial \kappa}{\partial \rho} \right)_{\sigma_{\min.}=0} = - \frac{\left(\frac{\partial \sigma_{\min.}}{\partial \rho} \right)_{\kappa}}{\left(\frac{\partial \sigma_{\min.}}{\partial \kappa} \right)_{\rho}} \geq 0. \quad (6.41)$$

The color-flavor locked condensate corresponds to $u = v$ and the difference $u - v$ represents one component of the octet under a simultaneous color-flavor rotation. Numerical solution to the equations of motion shows that this octet component does show up near the interface while the CFL condensate occupies the bulk $x > 0$. For weak coupling, ($\rho = -\frac{1}{2}$) we find that [42]

$$\kappa_c \simeq 0.589. \quad (6.42)$$

In terms of the Ginzburg-Landau coefficients (6.10) for weak coupling, we have a type I color superconductor if

$$k_B T_c < 0.036 \sqrt{\alpha_S} \mu, \quad (6.43)$$

and a type II color superconductor otherwise, where $\alpha_S = \frac{g^2}{4\pi}$.

D. Derivation of the Ginzburg-Landau theory from QCD one-gluon exchange.

In this subsection, we shall sketch the main steps that lead to the Ginzburg-Landau free energy functional (6.4) with the coefficients given by (6.10) [25].

Starting from the path integral representation of the free energy of a quark matter,

$$\exp(-\beta F) = \int [dA][d\psi][d\bar{\psi}] e^{-S_E}, \quad (6.44)$$

where

$$S_E = \int_0^\beta d\tau \int d^3 \vec{r} \mathcal{L} \quad (6.45)$$

with \mathcal{L} the QCD Lagrangian (2.1). The color superconducting order parameter can be triggered by the external source

$$\Delta S = \sum_{\vec{k}, P, h} {}' \text{Tr} [J_{\vec{k}}^*(P) O_{\vec{k}}^h(P) + \bar{O}_{\vec{k}}^h(P) J_{\vec{k}}(P)], \quad (6.46)$$

where $O_{\vec{k}}^h(P)$ and $\bar{O}_{\vec{k}}^h(P)$ are the quark bilinear forms of helicity h , i.e.

$$[O_{\vec{k}}^h(P)]_{f_1 f_2}^{c_1 c_2} = a_{f_2, h}^{c_2}(-P^-) a_{f_1, h}^{c_1}(P^+) \quad (6.47)$$

and

$$[\bar{O}_{\vec{k}}^h(P)]_{f_1 f_2}^{c_1 c_2} = \bar{a}_{f_1, h}^{c_1}(P^+) \bar{a}_{f_2, h}^{c_2}(-P^-). \quad (6.48)$$

with the color-flavor indices suppressed in (6.46) and the trace Tr is defined the same way as for Ψ in the beginning of this section. The capital letter P^\pm denotes the four-momentum $(\pm\frac{\vec{k}}{2} + \vec{p}, -\nu)$. The Grassmann numbers a and \bar{a} are related to the quark field in the coordinate representation, ψ and $\bar{\psi}$ through

$$\begin{aligned} a_{f,h}^c(P) &= \sqrt{\frac{1}{\beta\Omega}} \int_0^\beta d^3\vec{r} e^{-i(\vec{p}\cdot\vec{r} + \nu\tau)} u_h^\dagger(\vec{p}) \psi_{f,h}^c(\vec{r}, \tau) \\ \bar{a}_{f,h}^c(P) &= \sqrt{\frac{1}{\beta\Omega}} \int_0^\beta d^3\vec{r} e^{i(\vec{p}\cdot\vec{r} + \nu\tau)} \bar{\psi}_{f,h}^c(\vec{r}, \tau) u_h(\vec{p}) \end{aligned} \quad (6.49)$$

with $u_h(\vec{p})$ the positive energy solution to the Dirac equation of helicity h . The summation over the four momentum P in (6.46) extends only half \vec{p} -space. The pairing involving antiquarks is neglected.

Upon substitution of $S_E + \Delta S$ for S_E in (6.44), we have $F \rightarrow F + \Delta F$ with

$$\exp(-\beta\Delta F) = \frac{\int[dA][d\psi][d\bar{\psi}]e^{-S_E - \Delta S}}{\int[dA][d\psi][d\bar{\psi}]e^{-S_E}}. \quad (6.50)$$

Both ΔF and the induced order parameter

$$B_{\vec{k}}(P) = \frac{\int[dA][d\psi][d\bar{\psi}]O_{\vec{k}}^h(P)e^{-S_E - \Delta S}}{\int[dA][d\psi][d\bar{\psi}]e^{-S_E}} \quad (6.51)$$

and $B_K^*(P)$ can be expanded according to the powers of J and J^* . The Ginzburg-Landau free energy functional is obtained by the power series expansion of the Legendre transformation of ΔF ,

$$\Gamma = \Delta F - \frac{1}{\beta} \sum_{\vec{k}, P} \text{Tr}[J_{\vec{k}}^*(P) B_{\vec{k}}(P) + B_{\vec{k}}^*(P) J_{\vec{k}}(P)] \quad (6.52)$$

up to the forth power of $B_{\vec{k}}(P)$. Retaining only the color anti-triplet component of $B_{\vec{k}}(P)$, we find that [?]

$$\Gamma = \frac{1}{\beta} \sum_{P', P} \langle P' | \mathcal{M}_{\vec{k}} | P \rangle = \text{Tr} B_{\vec{k}}^\dagger(P) B_{\vec{k}}(P) + \frac{1}{2\beta} \sum_P [\nu^2 + (p - \mu)^2] \text{Tr}[B_{\vec{k}}^\dagger(P) B_{\vec{k}}(P)]^2, \quad (6.53)$$

where

$$\langle P' | \mathcal{M}_{\vec{k}} | P \rangle = -\mathcal{S}^{-1}(P^+) \mathcal{S}^{-1}(-P^-) \delta_{P', P} + \tilde{\Gamma}_{\frac{\vec{k}}{2}}(P' | P) \quad (6.54)$$

with $\mathcal{S}(P)$ the full quark propagator and $\tilde{\Gamma}_{\frac{\vec{k}}{2}}(P' | P)$ the 2PI vertex function for diquark scattering, all referring to positive energy states. The dependence of the quartic coefficient on the interactions and on the total momentum is neglected.

The kernel $\mathcal{M}_{\vec{k}}$ is isomorphic, upon multiplying the product of quark propagators on the right, to $1 - K_{\vec{q}, \delta}$ with $K_{\vec{q}, \delta}$ the kernel of the Dyson-Schwinger equation, eq.(5.10) at $\vec{q} = \frac{\vec{k}}{2}$ and $\delta = 0$. Introduce the normalized eigenfunction $u_{\vec{k}}(P)$ of $\mathcal{M}_{\vec{k}}$ with the minimum eigenvalue \mathcal{E} , i.e.

$$\frac{1}{\beta\Omega} \sum_{P'} \langle P | \mathcal{M}_{\vec{k}} | P' \rangle u_{\vec{k}}(P') = \mathcal{E} u_{\vec{k}}(P), \quad (6.55)$$

we have

$$\mathcal{E} = \frac{8\pi^2}{7\zeta(3)} k_B^2 T_c (T - T_c) + \frac{1}{6} k^2. \quad (6.56)$$

with T_c the same critical temperature determined before. Since the Ginzburg-Landau theory is expected to be valid when $|T - T_c| \ll T_c$ and the two terms on RHS of (6.56) becomes comparable, we have $k \ll k_B T_c$ and the angular momentum mixing discussed in the context of LOFF pairing, which occurs when $k \sim k_B T_c$, can be neglected.

On writing

$$B_{\vec{k}}(P) = \sqrt{6} \Psi_{\vec{k}} u_{\vec{k}}(P) \quad (6.57)$$

with

$$\Psi_{\vec{k}} = \frac{1}{\sqrt{\Omega}} \int d^3 \vec{r} e^{-i\vec{k} \cdot \vec{r}} \Psi(\vec{r}) \quad (6.58)$$

and substituting (6.57) to (6.53) we obtain the Ginzburg-Landau free energy functional (6.4) with the coefficients (6.10). The form of the gauge coupling is dictated by the requirement of gauge invariance.

The same expression of the Ginzburg-Landau coefficients in terms of μ and T would be obtained if the underlying dynamics is given by a NJL effective action.

VII. CONCLUDING REMARKS.

In this lecture, I have reviewed the perturbative aspect of the color superconductivity in the regime of asymptotic freedom. The approximations made so far are systematic and the result obtained are theoretically important. But there is not a known mechanism which can maintain a quark matter with a baryon density such that $\mu \gg \Lambda_{\text{QCD}}$ at equilibrium against gravitational collapse. In the core of a neutron star, the baryon density is not likely to exceed that of a normal nuclear matter by one order of magnitude and the corresponding chemical potential is speculated to be few hundreds of MeV. Taking $\mu = 400$ MeV and $\Lambda_{\text{QCD}} = 200$ MeV as a benchmark, we have $\alpha_S \equiv \frac{g^2}{4\pi} \simeq 1$. It follows from (2.8) for $N_c = N_f = 3$ and $J = 0$ that $T_c = 3.5$ MeV. The Ginzburg-Landau parameter falls in the type I region according to (6.43). But this estimations may subject significant corrections for the following reasons:

1. The higher order corrections:

The sub-sub-leading term of the perturbation series (3.1) takes the form $\lambda' g$ with the ansatz

$$\lambda' = c \ln g + c'. \quad (7.1)$$

The first term remains infrared, but the second term entails a matching between the infrared contributions to ultraviolet ones and the result depends on the definition of g . It is important to notice that the diagrams which seems contributing according to explicit powers of g turns out not so if there is no forward singularity. The crossed box diagram discussed in subsection IV.E is an example. While it will take major efforts to collect all contributions to the coefficients c and c' , some of them can be obtained readily and their magnitudes serve as a clue to the accuracy of the perturbative expansion when extrapolated to the realistic baryon density. One contribution to c comes from the coupling constant g under the non Fermi liquid logarithm of the quark-self energy. In terms of the scaled Matsubara energy $\hat{\nu}$, the logarithm of ΔK in the subsection IV.B becomes

$$\ln \frac{1}{\hat{\nu}} + 3g + \text{const.} \quad (7.2)$$

Following the same steps there, the second term contributes to c a term $\frac{1}{4\sqrt{3}}$. A contribution to c' comes from the quasi-particle damping rate and has been calculated in [17]. It contributes to c' a term equal to $\frac{1}{6\sqrt{2}}$. Including these two corrections only, the transition temperature may be written as

$$k_B T_c = 512 \left(\frac{2}{N_f} \right)^{\frac{5}{2}} \frac{\mu}{g_{\text{eff.}}^{5 + \frac{1}{4\sqrt{3}} g_{\text{eff.}}}} e^{-\frac{3\pi^2}{\sqrt{2}g_{\text{eff.}}} - \frac{\pi^2 + 4}{8}}, \quad (7.3)$$

for $N_c = 3$, where

$$g_{\text{eff.}}^2 = g^2 \left(1 - \frac{1}{9\pi^2} g^2 \right). \quad (7.4)$$

The instanton mediated pairing force considered in subsection II. A, which is suppressed in the region of asymptotic freedom may come to play significant roles for the realistic baryon density. Recently the author of [44] found that the gap energy produced by the one-gluon exchange and the instanton induced pairing force is considerably enhanced for a moderate chemical potential relative to that given by the one-gluon exchange alone.

2. Exotic pairing state

At an intermediate chemical potential, say $\mu = 400\text{MeV}$ the quark masses and their difference among different flavors has to be ignored. Because of the large mass of s quark and the restriction of charge neutrality, we are in the situation of two flavor pairing in a mismatched Fermi sea. One candidate is the LOFF pairing discussed in section V, which gives rise to a crystalline structure of the long range order and may shed new lights on the glitching phenomena of a neutron star [34]. The other possibility is spin-one pairing between two quarks of the same flavor, which does not suffer from the mismatch [23]. The energy scale of spin-one pairing is, however very low, of the order of keV and it may occur in the late stage of the cooling history of a neutron star [20].

A potential competing pairing state is the gapless superconductivity suggested recently [45] [46] [47]. In the presence of a Fermi momentum difference δ (defined in section V) of pairing quarks, the solution to the gap equation with zero net momentum, plotted against δ , contains two branches. One of them, with $\Delta > \delta$, gives rise to gapped excitation spectrum as usual and the other branch, with $\Delta < \delta$, gives rise to gapless spectrum. Regarding the

free energy as a function of the gap parameter Δ , and δ , the solutions along the second branches are saddle points and the corresponding state is unstable without constraints. But as shown in [47] for NJL effective action with moderate pairing strength, the constraint of charge neutrality, however corresponds to a trajectory on $\Delta - \delta$ plane that intersects the gapless branch only. The free energy is minimized at the gapless solution of the gap equation along the trajectory of charge neutrality. The thermodynamics of this pairing state is largely characterized by the gapless feature of the excitations.

Color superconductivity continues to be an active field of research. There are many theoretical issues still to be addressed. The experimental confirmation its existence depends on the progresses along the following three avenues: 1) A robust extrapolation of the first principle calculations to moderate chemical potential by incorporating nonperturbative effects. 2) A practical simulation method that can handle the fermion sign problem. 3) A list of clear cut signals to identify CSC phase in a compact stellar objects. With joint efforts of high energy physicists, nuclear physicists and astrophysicists, it is quite feasible that a much deeper insight can be gained on the high density area of the QCD phase diagram in near future.

VIII. ACKNOWLEDGMENTS

I am grateful to W. Brown, I. Giannakis and J. T. Liu for collaborations which resulted in the works reported here. I am indebted to D. Rischke for a discussion that motivated my derivation of the group theoretic factor (2.4) for pairing with arbitrary representations of quarks. I would also like to extend my gratitude to Mei Huang and I. Shovkovy for a detailed explanation on the gapless color superconductivity and to De-fu Hou, D. Rischke and Qun Wang for discussions on the gauge invariance in the super phase during my visit at the University of Frankfurt. Finally, but not the least, I would like to thank Professors Wei-qin Chao, Peng-fei Zhuang and the staffs of China Center of Advanced Science and Technology (CCAST) for organizing this exciting workshop on color superconductivity. This research is supported in part by US Department of Energy contract number DE-FG02-91ER40651-TASKB.

APPENDIX A

In this appendix, we shall derive the formula for the group theoretic factor of the scattering amplitude of two quarks via one-gluon exchange process specific to an irreducible representation of di-quark system. Each of them can be in any irreducible representation of the gauge group.

Denoting the representation space of the two interacting quarks by R_1 and R_2 , the product of which can be decomposed into a number of irreducible representations, say R 's. The group theoretic factor associated to the one-gluon exchange diagram specific to a particular di-quark representation, R is an eigenvalue of the operator $T_1^c T_2^c$ which acts in the product space $R_1 \otimes R_2$, where

$$T_1^c = T_{R_1}^c \otimes 1 \quad (\text{A1})$$

and

$$T_2^c = 1 \otimes T_{R_2}^c \quad (\text{A2})$$

with T_R^c the generator of the representation R . The negative eigenvalue gives rise to pairing while the positive one to repulsion. As only the quadratic form of the generators is involved, we may follow the same methodology of diagonalizing the scalar product of two angular momentum of $SU(2)$ group, which amounts to

$$\vec{J}_1 \cdot \vec{J}_2 = \frac{1}{2}(\vec{J}^2 - \vec{J}_1^2 - \vec{J}_2^2) = \frac{1}{2}[J(J+1) - J_1(J_1+1) - J_2(J_2+1)] \quad (\text{A3})$$

with $\vec{J} = \vec{J}_1 + \vec{J}_2$.

The group generator in the product space $R_1 \otimes R_2$ is

$$T^c = T_1^c + T_2^c \quad (\text{A4})$$

A decomposition parallel to (A3) reads

$$T_1^c T_2^c = \frac{1}{2}[T^c T^c - T_1^c T_1^c - T_2^c T_2^c] \quad (\text{A5})$$

and the eigenvalue of the operator $T_1^c T_2^c$ specific to the diquark representation R is

$$\frac{1}{2}(C_R - C_{R_1} - C_{R_2}) \quad (\text{A6})$$

with C_R the second Casimir in the irreducible representation R .

APPENDIX B

In this appendix, we shall evaluate explicitly the Fredholm determinant pertaining to the integral equation (2.9), i.e.

$$\mathcal{D} = \sum_0^{\infty} (-)^n k^{2n} \mathcal{D}_n, \quad (\text{B1})$$

where

$$\mathcal{D}_n = \frac{1}{n!} \int_a^b dx_n \dots \int_a^b dx_1 D_n(x_1, \dots, x_n) \quad (\text{B2})$$

with $D_n(x_1, \dots, x_n)$ the determinant

$$D_n(x_1, \dots, x_n) = \begin{vmatrix} x_1 & \min(x_1, x_2) & \min(x_1, x_3) & \dots & \min(x_1, x_n) \\ \min(x_2, x_1) & x_2 & \min(x_2, x_3) & \dots & \min(x_2, x_n) \\ \min(x_3, x_1) & \min(x_3, x_2) & x_3 & \dots & \min(x_3, x_n) \\ \dots & \dots & \dots & \dots & \dots \\ \min(x_n, x_1) & \min(x_n, x_2) & \min(x_n, x_3) & \dots & x_n \end{vmatrix}. \quad (\text{B3})$$

In terms of the variables

$$\xi_j = \frac{x_j - a}{b - a}, \quad (B4)$$

we have

$$\mathcal{D}_n = (b - a)^n I_n + a(b - a)^{n-1} J_n, \quad (B5)$$

where

$$I_n = \frac{1}{n!} \int_0^1 d\xi_n \dots \int_0^1 d\xi_1 D_n(\xi_1, \dots, \xi_n) \quad (B6)$$

and

$$J_n = \frac{1}{(n-1)!} \int_0^1 d\xi_n \dots \int_0^1 d\xi_1 D_n^1(\xi_1, \dots, \xi_n). \quad (B7)$$

with $D_n^1(\xi_1, \dots, \xi_n)$ the determinant of the matrix obtained from $D_n(\xi_1, \dots, \xi_n)$ upon replacing its elements of the first column by ones, i.e.

$$D_n^1(\xi_1, \dots, \xi_n) = \begin{vmatrix} 1 & \min(\xi_1, \xi_2) & \min(\xi_1, \xi_3) & \dots & \min(\xi_1, \xi_n) \\ 1 & \xi_2 & \min(\xi_2, \xi_3) & \dots & \min(\xi_2, \xi_n) \\ 1 & \min(\xi_3, \xi_2) & \xi_3 & \dots & \min(\xi_3, \xi_n) \\ \dots & \dots & \dots & \dots & \dots \\ 1 & \min(\xi_n, \xi_2) & \min(\xi_n, \xi_3) & \dots & \xi_n \end{vmatrix}. \quad (B8)$$

The permutation symmetry of the integral with respect to x_1, \dots, x_n is employed in deriving (B5) from (B2).

To evaluate I_n , we order the integration variables such that $\xi_1 < \xi_2 < \dots < \xi_n$. We find that

$$D_n(\xi_1, \dots, \xi_n) = \begin{vmatrix} \xi_1 & \xi_1 & \xi_1 & \dots & \xi_1 \\ \xi_1 & \xi_2 & \xi_2 & \dots & \xi_2 \\ \xi_1 & \xi_2 & \xi_3 & \dots & \xi_3 \\ \dots & \dots & \dots & \dots & \dots \\ \xi_1 & \xi_2 & \xi_3 & \dots & \xi_n \end{vmatrix}. \quad (B9)$$

Multiplying the second column by $\frac{\xi_1}{\xi_2}$ and subtract the result from the first column, we obtain the relation

$$D_n(\xi_1, \xi_2, \dots, x_n) = \xi_1 \left(1 - \frac{\xi_1}{\xi_2}\right) D_{n-1}(\xi_2, \dots, \xi_n) \quad (B10)$$

Recursively, we end up with

$$D_n(\xi_1, \dots, \xi_n) = \prod_{j=1}^n \xi_j \prod_{j=1}^{n-1} (\xi_{j+1} - \xi_j). \quad (B11)$$

Introduce a new set of integration variables

$$\begin{aligned}
\xi_1 &= \eta_1 \eta_2 \dots \eta_n \\
\xi_2 &= \eta_2 \eta_3 \dots \eta_n \\
&\dots \dots \dots \\
\xi_n &= \eta_n
\end{aligned} \tag{B12}$$

we have

$$I_n = \int_0^1 \prod_{j=1}^n \xi_n^{2n-1} \prod_{j=1}^{n-1} \xi_j^{2j-1} (1 - \xi_j) = \frac{1}{(2n)!}. \tag{B13}$$

To evaluate J_n , we order the integration variables such that $\xi_2 < \dots < \xi_n$. Following the same treatment of D_n , we find $D_n^1(\xi_1, \xi_2, \dots, \xi_n) = 0$ if $\xi_1 > \xi_2$ and

$$D_n^1(\xi_1, \dots, \xi_n) = \frac{D_n(\xi_1, \dots, \xi_n)}{\xi_1} \tag{B14}$$

if $\xi_1 < \xi_2$. In terms of the new variables (B12), we end up with

$$J_n = \frac{1}{(2n-1)!}. \tag{B15}$$

Substituting (B13), (B15) and (B5) to (B1) we obtain that

$$\mathcal{D} = \cos k(b-a) - ka \sin k(b-a), \tag{B16}$$

which gives rise to the same eigenvalue condition as (3.43).

APPENDIX C

In this appendix, we shall discuss the color sextet component of the condensate. Upon decomposing the diquark condensate into color $\bar{\mathbf{3}}$ component ϕ , and $\mathbf{6}$ component χ ,

$$\Psi = \phi + \chi \tag{C1}$$

the quadratic term of the Ginzburg-Landau free energy takes the form

$$\Gamma_2 = \text{Tr}(a\phi^\dagger\phi + a'\chi^\dagger\chi) \tag{C2}$$

with $a = \bar{a}(T - T_c)$ and $a' > 0$. The quartic term Γ_4 contains all possible combinations of ϕ and χ that is invariant under the symmetry group (2.19). Among these combinations, there exists a term of the form $\chi^*\phi^*\phi\phi$ and its complex conjugate. Indeed, it follows from the decomposition rules of $SU(3)$ group

$$\begin{aligned}
\mathbf{3} \otimes \mathbf{3} &= \bar{\mathbf{3}} \oplus \mathbf{6} \\
\bar{\mathbf{3}} \otimes \bar{\mathbf{3}} &= \mathbf{3} \oplus \bar{\mathbf{6}} \\
\mathbf{6} \otimes \bar{\mathbf{3}} &= \mathbf{3} \oplus \mathbf{15}
\end{aligned} \tag{C3}$$

that the product representation of $\phi^* \phi \phi$ consists of one $\bar{\mathbf{6}}$ which forms an invariant with χ . Since this term is linear in χ , a nonzero expectation value of χ will be induced by a nonzero value of ϕ upon minimizing the Ginzburg-Landau free energy at $T < T_c$ and its contribution to the free energy in the super phase is smaller than that of the anti-triplet by one power of $\frac{T_c - T}{T_c}$. For the Ginzburg-Landau coefficient in the weak coupling, (6.10), we find that the sextet component of the condensate corrects the bulk free energy density by the amount

$$\frac{\Delta\Gamma_{\min.}}{\Omega} = -\frac{558\zeta(5)}{343\zeta^3(3)}\mu^2 k_B^2 T_c^2 \left(\frac{T_c - T}{T_c}\right)^3. \quad (\text{C4})$$

REFERENCES

- [1] B. Barrois, Nucl. Phys. **B129** (1977) 390.
- [2] S. Frautschi, *Proceedings of the Workshop on Hadronic Matter at Extreme Energy Density*, N. Cabibbo, ed., Erice, Italy (1978).
- [3] D. Bailin and A. Love, Phys. Rep. **107** (1984) 325.
- [4] M. Alford, K. Rajagopal and F. Wilczek, Phys. Lett. **B422** 247 (1998).
- [5] R. Rapp, T. Schaefer, E. V. Shuryak, M. Velkovsky, Phys. Rev. Lett. **81** (1998) 53.
- [6] M. Alford, K. Rajagopal and F. Wilczek, Nucl. Phys. **B537**, 443 (1999).
- [7] M. Gyulassy, nucl-th/0403032.
- [8] D. T. Son, Phys. Rev. **59**, (1999) 094019.
- [9] T. Schaefer and F. Wilczek, Phys. Rev. **D60**, 114033 (1999).
- [10] R. Pisarski and D. Rischke, Phys. Rev. Lett. **83** 37 (1999).
- [11] R. Pisarski and D. Rischke, Phys. Rev. **D61** 051501 (2000).
- [12] D. K. Hong, Phys. Lett. **B473** 118 (2000).
- [13] D. K. Hong, V. A. Miransky, I. A. Shovkovy and C. R. Wijewardhana, Phys. Rev. **D61**, 056001 (2000).
- [14] W. Brown, J. T. Liu and H. C. Ren, Phys. Rev. **D61**, 114012 (2000).
- [15] W. Brown, J. T. Liu and H. C. Ren, Phys. Rev. **D62**, 054016 (2000).
- [16] W. Brown, J. T. Liu and H. C. Ren, Phys. Rev. **D62**, 054013 (2000).
- [17] C. Manuel, Phys. Rev. **D62** 114008, (2000).
- [18] Q. Wang and D. Rischke, Phys. Rev. **D65** 054005 (2002).
- [19] De-fu Hou, Qun Wang and D. Rischke, hep-ph/0401152.
- [20] K. Rajagopal and F. Wilczek, hep-ph/0011333, in *At the Frontier of Particle Physics/Handbook of QCD*, B. L. Ioffe Festschrift, edited by M. Shifman (World Scientific, Singapore); M. Alford, Ann. Rev. Nucl. Part. Sci., **51**, 131 (2001); T. Schaefer, hep-ph/0304281; D. Rischke, Prog Part. Nucl. Phys. **52** 197(2004); R. Casalbuoni and G. Nardulli, hep-ph/0305069.
- [21] 't Hooft, Phys. Rev. **D14**, 3432 (1976).
- [22] M. Shifman, A. J. Vainshtein and V. I. Zakharov, Nucl. Phys. **B163**, 46 (1980); E. Shuryak, Nucl. Phys. **B203**, 140 (1982); D. I. Diakonov and V. Y. Petrov, Nucl. Phys. **B245**, 259 (1984).
- [23] T. Schaefer, Phys. Rev. **D62**, 094007 (2000). A. Schmitt, Qun Wang and D. Rischke, Phys. Rev. Lett., **91**, 242301 (2003).
- [24] T. Schaefer, Nucl. Phys. **B575**, 269 (2000); I. Shovkovy and L. C. Wijewardhana, Phys. Lett. **470B**, 189 (1999).
- [25] I. Giannakis and H. C. Ren, Phys. Rev. **D65** 054017 (2002).
- [26] M. Alford, J. Berges and K. Rajagopal, Nucl. Phys. **B571** (2000).
- [27] K. Rajagopal and F. Wilczek, Phys. Rev. Lett. **86**, 3492 (2001).
- [28] D. T. Son and M. A. Stephanov, Phys. Rev. **D61**, 074012 (2000); **D62**, 059902 (2000).
- [29] C. Manuel and M. H. G. Tytgat, Phys. Lett. **B479**, 190 (2000)
- [30] M. Le Bellac, *Thermal Field Theory* (Cambridge University Press, Cambridge, England, 1996).
- [31] E. T. Whittaker and G. N. Watson, *A Course of Modern Analysis*, 4th ed. (Cambridge University Press, Cambridge, England, 1962).

- [32] T. Holstein, R. E. Norton and P. Pincus, Phys. Rev. **B6** 2649(1973); M. Yu. Reizer, Phys. Rev. **B40**, 11571(1988), Phys. Rev. **B44**, 5476(1991).
- [33] T. Schaefer, Nucl. Phys. **A728** 251(2003).
- [34] J. A. Bowers, J. Kundu, K. Rajagopal and E. Shuster, Phys. Rev. **D64**, 014024 (2001).
- [35] A. J. Larkin and Yu. N. Ovchinnikov, Zh. Eksp. Teor. Fiz. **47** 1136(1964) (Soviet Physics JETP **20** 762(1965); P. Fulde and R. A. Ferrell, Phys. Rev. **135** A550(1964).
- [36] S. Takada and T. Izuyama, Prog. Theor. Phys. **41** 635(1969).
- [37] A. K. Leibovich, K. Rajagopal and E. Shuster, Phys. Rev. **D64**, 094005 (2001).
- [38] I. Giannakis, J. T. Liu and H. C. Ren, Phys. Rev. **D66** 031501 (2002).
- [39] J. Bowers and K. Rajagopal, Phys. Rev. **D66** 065002 (2002).
- [40] V. L. Ginzburg and L. D. Landau, Zh. Eksp. Teor. Fiz. **20** 1064 (1950).
- [41] K. Iida and G. Baym, Phys. Rev. **D63** 074018 (2001); Phys. Rev. **D66** 014015 (2002).
- [42] I. Giannakis and H. C. Ren, Nucl. Phys. **B669** 462 (2003).
- [43] A. A. Abrikosov, Soviet Physics JETP **5** 1174 (1957).
- [44] T. Schaefer, hep-ph/0402032.
- [45] W. V. Liu and F. Wilczek, Phys. Rev. Lett. **90** 047002 (2003).
- [46] Mei Huang, Pengfei Zhuang and Weiqin Chao, Phys. Rev. **D67**, 065051 (2003).
- [47] I. Shovkovy and Mei Huang, Phys. Lett. **B564**, 205 (2003); Nucl. Phys. **A729**, 835 (2003).